RNA-Cleaving DNA Enzymes and Their Potential Therapeutic Applications as Antibacterial and Antiviral Agents

P.I. Pradeepkumar and Claudia Höbartner

Contents

Abstract DNA catalysts are synthetic single-stranded DNA molecules that have been identified by in vitro selection from random sequence DNA pools. The most prominent representatives of DNA catalysts (also known as DNA enzymes, deoxyribozymes, or DNAzymes) catalyze the site-specific cleavage of RNA substrates. Two distinct groups of RNA-cleaving DNA enzymes are the 10-23 and 8-17 enzymes. A typical RNA-cleaving DNA enzyme consists of a catalytic core and two short binding arms which form Watson–Crick base pairs with the

P.I. Pradeepkumar (✉)
Department of Chemistry, Indian Institute of Technology Bombay, Powai, Mumbai 400076, India
e-mail: pradeep@chem.iitb.ac.in

C. Höbartner (✉)
Max Planck Institute for Biophysical Chemistry, Research Group Nucleic Acid Chemistry, Am Fassberg 11, 37077 Göttingen, Germany
e-mail: claudia.hoebartner@mpibpc.mpg.de

V.A. Erdmann and J. Barciszewski (eds.), *From Nucleic Acids Sequences to Molecular Medicine*, RNA Technologies, DOI 10.1007/978-3-642-27426-8_15,

RNA targets. RNA cleavage is usually achieved with the assistance of metal ions such as Mg^{2+}, Ca^{2+}, Mn^{2+}, Pb^{2+}, or Zn^{2+}, but several chemically modified DNA enzymes can cleave RNA in the absence of divalent metal ions. A number of studies have shown the use of 10-23 DNA enzymes for modest downregulation of therapeutically relevant RNA targets in cultured cells and in whole mammals. Here we focus on mechanistic aspects of RNA-cleaving DNA enzymes and their potential to silence therapeutically appealing viral and bacterial gene targets. We also discuss delivery options and challenges involved in DNA enzyme-based therapeutic strategies.

Keywords Antibacterials • Antivirals • Catalyst • Chemical modification • Delivery • Deoxyribozyme • DNA enzyme • Gene silencing • In vitro selection • Mutation • RNA cleavage

1 Introduction

The conventional biological role of both DNA and RNA as storage place and carrier of genetic information has taken a new leap in the early 1980s by the seminal discovery of RNA catalysts, called ribozymes, by Cech and Altman (Kruger et al. 1982; Guerrier-Takada et al. 1983). Ever since these reports, there has been a surge of new discoveries in this research area, and as a result, new functional roles of nucleic acids have emerged, including their involvement in gene regulation (Breaker 2004). Many ribozymes have been found in biological systems catalyzing important biochemical reactions, which include splicing of mRNAs (Doudna and Cech 2002) and peptide bond formation at the core of the ribosome (Leung et al. 2011). Moreover, a number of ribozymes with a wide variety of functions have been discovered in the laboratory using an elegant test tube evolution method called in vitro selection (Joyce 2007). These discoveries also shook the notion that not only proteins but also nucleic acids can function as catalysts with high precision and impressive rate enhancements. The ability of RNA to catalyze a particular reaction is aided by its propensity to fold and adopt defined 3D structures and thereby facilitate metal ion or cofactor-assisted catalysis (Lilley 2011). After the discovery of ribozymes, the possibility of the existence of DNA catalysts based on single-stranded DNAs was speculated the mid-1980s (Kruger et al. 1982), but no such catalysts have yet been found in any domains of life. In 1994, the first DNA catalyst was discovered in the laboratory using in vitro selection. Single-stranded DNA was shown to site-specifically cleave an RNA phosphodiester bond with the assistance of Pb^{2+} ions (Breaker and Joyce 1994).

The unique ability of single-stranded DNA to catalyze RNA cleavage prompted researchers to capitalize on the catalytic potential of DNA. Since DNA, unlike RNA, lacks a 2′-OH group and bears a 5-methyl group in uridine (i.e., thymidine), a question that remained to be answered was if DNA has the ability to achieve the catalytic diversity exhibited by ribozymes. Later in vitro selection experiments have shown ample evidence that DNA catalysis is not limited by the chemistry of the

reaction but rather by the techniques involved to identify active DNA sequences. As a consequence, in addition to a series of RNA-cleaving enzymes, new DNA catalysts have been identified in a number of laboratories. These include DNA enzymes, which are capable of performing oxidative and hydrolytic cleavage of DNA (Carmi et al. 1998, Chandra et al. 2009), DNA phosphorylation (Li and Breaker 1999), DNA adenylation (Li et al. 2000b), phosphoramidate cleavage (Burmeister et al. 1997), peroxidation (Travascio et al. 1998), thymine dimer cleavage (Chinnapen and Sen 2004), porphyrin metalation (Li and Sen 1996), formation of phosphorothioester linkage (Levy and Ellington 2001), linear RNA ligation (formation both 2′–5′ and 3′–5′ linkages) (Purtha et al. 2005; Kost et al. 2008), synthesis of 2′,5′-branched nucleic acids (Coppins and Silverman 2004; Lee et al. 2011), lariat RNA synthesis (Wang and Silverman 2005), DNA depurination (Sheppard et al. 2000; Höbartner et al. 2007), formation of nucleopeptide linkages (Pradeepkumar et al. 2008) and nucleopeptides (Wong et al. 2011), and C–C bond formation (Diels–Alder reaction) (Chandra and Silverman 2008). Moreover, the search for new catalytic activities of DNA is currently actively being pursued in many laboratories. To gather detailed information on DNA catalysis and various reactions catalyzed by DNA, the reader is directed to excellent recent reviews published elsewhere (Silverman 2008, 2009, 2010; Schlosser and Li 2009a; Willner et al. 2008).

The focus of this chapter is the most widely studied class of deoxyribozymes, namely, RNA-cleaving DNA enzymes. These enzymes find broad applications not only in the conventional laboratory settings to manipulate large RNAs (Pyle et al. 2000; Silverman and Baum 2009) but also in the field of chemical sensing (Willner et al. 2008) and in the therapeutic arena, where they have shown the potential to downregulate gene expression (Baum and Silverman 2008). RNA-cleaving DNA enzymes offer specific advantages over RNA-cleaving ribozymes due to their chemical stability, easy accessibility by chemical solid-phase synthesis, and cost-effectiveness. The two major classes of RNA-cleaving enzymes are 10-23 and 8-17, both of which have been widely used in the above-mentioned applications. Both of these enzymes have a short catalytic core of 13–15 nt and recognize the target RNA sequence with the binding arms through Watson–Crick base pairing. Both enzymes require mostly divalent metal cations such as Mg^{2+}, Mn^{2+}, Zn^{2+}, Ca^{2+}, etc., for achieving efficient catalysis. Under optimized conditions, the 10-23 DNA enzyme exhibits k_{cat}/K_m of 10^9, which rivals the catalytic efficiency of ribozymes such as the hammerhead ribozyme and protein enzymes such as RNase A (Santoro and Joyce 1998). This fact underscores the robustness of DNA catalysis and provides opportunities to harness the catalytic activities of DNA for practical applications. Herein we review in vitro selection techniques used to identify RNA-cleaving DNA enzymes and summarize kinetic and mechanistic insights on the RNA cleavage reaction revealed by various biochemical and biophysical studies. Further, we give an overview on the potential use of RNA-cleaving DNA enzymes in the therapeutic area, where the focus is devoted to bacterial and viral targets.

2 In Vitro Selection Strategies

RNA-cleaving DNA enzymes are selected or evolved from a random library of DNA sequences (DNA pool) through repeated steps of selection and amplification (Joyce 2004). The subtle difference between in vitro *selection* and in vitro *evolution* techniques should be noted. If the process involves the identification of enzymes from the initial library of sequences without introducing genetic diversity between individual rounds of selective amplification, the procedure is called in vitro *selection*. However, if additional diversity is introduced, for example, using error-prone PCR during the selection process or a reselection is carried out using partially randomized libraries (based on the sequence information emerged from the initial selection), the process is called in vitro *evolution*. The random library is usually constructed by solid-phase DNA synthesis using a mixture of all four phosphoramidites in appropriate ratios based on their coupling efficiency (T > G > C > A). The DNA pool is generally designed with two well-defined primer binding sites, which enable PCR amplification after the selection step, and a random region, which usually varies from 20 to 80 nt in length. The length of the random region defines the sequence space (i.e., all possible sequences for a random region of length $n = 4^n$). For example, a random region of 40 nt has a sequence space of $4^{40} = 10^{24}$ sequences, which is impossible to sample experimentally due to practical limitations. To illustrate this, a 60-nt-long DNA pool containing 40 random nucleotides would require 1.6 mols of DNA, i.e., 30 kg, in order to achieve complete coverage of all 10^{24} possible sequences. In practice, typically 0.2–2 nanomoles of DNA pool is used to initiate the selection. This accounts to 10^{14}–10^{15} different molecules, which offer a sampling of only 10^{-9}–10^{-10} (e.g., $10^{14}/10^{24} = 10^{-10}$) of the sequence space. Increasing the length of the random region therefore leads to a decrease in the coverage of sequence space [for a detailed discussion, see Silverman (2008)]. A number of selection experiments have shown that a very large random region is not required to identify efficient DNA catalysts with a wide variety of functions (Silverman 2008; Schlosser and Li 2009a).

Two strategies for the in vitro selection process employed to identify RNA-cleaving DNA enzymes are shown in Fig. 1, termed "bead-based" and "gel-based" strategies (Santoro and Joyce 1997; Cruz et al. 2004). One of the crucial steps in this process is the physical separation of active DNA molecules from inactive ones. In the bead-based approach, this is usually accomplished by the help of a biotin tag which assists in retaining the inactive sequences on a streptavidin column after cleavage of the target RNA in the selection step (Fig. 1a). More stringent separations can be achieved in the gel-based approach, where the active enzymes are separated based on their different mobility in denaturing PAGE due to the size difference imparted during the cleavage step (Fig. 1b). These methods demand that the substrate and the DNA pool are covalently joined together at the beginning of the selection experiment. Therefore, in the first step of a selection cycle, the DNA pool is attached to an RNA substrate (or to a DNA containing an embedded ribonucleotide) either by performing PCR using a biotinylated primer or by enzymatic ligation (using T4 DNA or T4 RNA ligase). This is followed by the selection

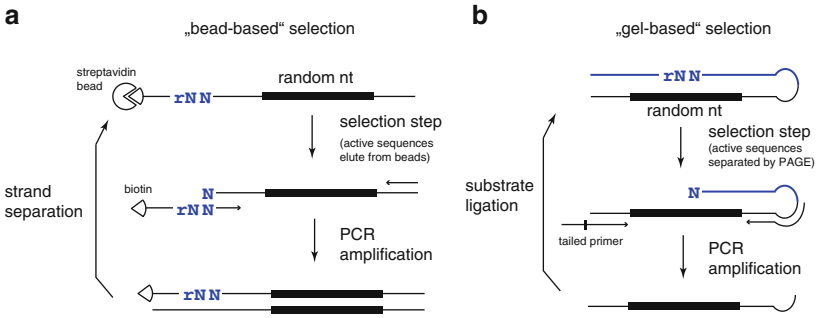

Fig. 1 In vitro selection strategies for RNA-cleaving deoxyribozymes. (**a**) "Bead-based" selection via biotin–streptavidin interaction. (**b**) "Gel-based" selection via PAGE separation. See text for details

step in which parameters such as buffer, pH, temperature, metal ion concentration, and incubation time are varied to set up different selection experiments in order to identify the most efficient DNA enzymes. The selection step is followed by fishing out the active DNA enzyme sequences using the methods described above. Then, the selected sequences are PCR amplified using appropriate primers. If the separation is carried out using the bead-based approach, the biotinylated primer will enable the capture of PCR product on the streptavidin column. A denaturation step is then performed to remove the undesired complementary strand of the double-stranded PCR product. If the separation involves a gel-based strategy, a reverse primer with an embedded ribonucleotide or a nonamplifiable linker is used. This provides the opportunity to generate a size difference in the amplified products required for PAGE-based separation of single-stranded DNA. This is achieved either by cleaving the ribonucleotide linkage or by utilizing the inherent difference in the size of the two strands. The selection and amplification steps are continued until no further increase in cleavage activity is observed. This typically requires between 5 and 15 round of in vitro selection. The individual sequences are then identified by the typical cloning and automated sequencing procedures. The cleavage activity of individual deoxyribozymes is analyzed by using solid-phase synthesized oligonucleotides that bind to the target RNA in a bimolecular format. This is usually referred to as "in trans" assay format, compared to the monomolecular "in cis" architecture used during selection.

3 RNA-Cleaving Deoxyribozymes: A Brief Overview

The chemical reaction catalyzed by all known RNA-cleaving deoxyribozymes is the formation of a 2′,3′-cyclic phosphate and a free 5′-hydroxyl terminus, originating from the nucleophilic attack of a 2′-hydroxyl group of the substrate

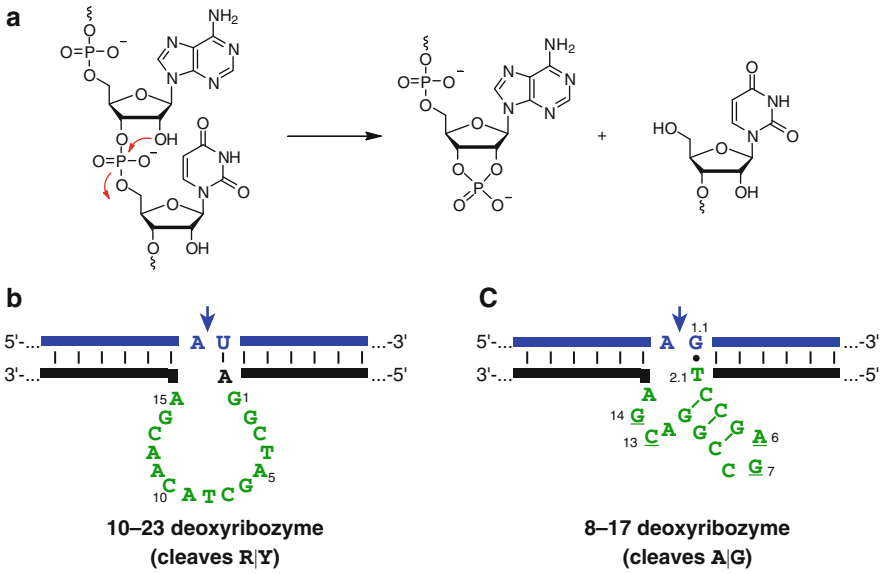

Fig. 2 (**a**) DNA-catalyzed RNA cleavage. Nucleophilic attack of the 2′-OH group onto the adjacent phosphodiester bond generates a 2′,3′-cyclic phosphate and a free 5′-OH terminus. (**b**) 10-23 deoxyribozyme. (**c**) 8-17 deoxyribozyme; conserved nucleotides most important for cleavage activity are *underlined*. The preferred cleavage sites are indicated by *blue arrows*

oligonucleotide on the adjacent phosphodiester bond (Fig. 2a). In principle, such an intramolecular cleavage reaction can occur randomly upon incubation of RNA under alkaline conditions. Deoxyribozymes, however, specifically cleave RNA only at predefined internal positions under mild conditions. The site specificity is programmed via the Watson–Crick base-paired binding arms, which generally leave 1 nt at the target site unpaired. The considerable rate enhancements and extremely high selectivities for particular sites render deoxyribozymes attractive tools for various applications.

The first reported deoxyribozyme catalyzed the cleavage of the phosphodiester bond on the 3′-side of single embedded ribonucleotide in a DNA substrate by using Pb^{2+} as a divalent metal ion cofactor (Breaker and Joyce 1994). At pH 7.0 and 23°C, in the presence of 1 mM $Pb(OAc)_2$, the DNA catalyst was able to cut its substrate in a bimolecular fashion and showed impressive Michaelis–Menten behavior, with k_{cat} of 1 min^{-1} and K_m of 2 μM, yielding ca. 30 turnovers per hour at a catalyst concentration of 0.01 μM and a substrate concentration of 1 μM. The rate enhancement over the uncatalyzed background reaction (10^{-4} min^{-1}) under comparable conditions amounts to 10^5. Although this initially reported deoxyribozyme was not capable of cleaving an all-RNA substrate, this prototype DNA catalyst spurred the development of successor deoxyribozymes that now offer highly useful properties.

Table 1 Representative examples of RNA phosphodiester-cleaving deoxyribozymes (consisting of unmodified DNA)

Deoxyribozyme name	Preferred cleavage site[a]	Random pool (nt)	Required cofactor (s)	max k_{obs} (min^{-1})	Rate enhancement	References
Pb^{2+}-depend.	alG	50	Pb^{2+}	1	~10^5	Breaker and Joyce (1994)
E6	n.k.	40	Mg^{2+}	0.04	10^5	Breaker and Joyce (1995)
Na8	n.k.	40	Na^+	0.007	10^8	Geyer and Sen (1997)
HD2	alG	40	L-histidine	0.2	10^6	Roth and Breaker (1998)
Mg5 (8-17 variant)	alG	74	Ca^{2+}	0.1		Faulhammer and Famulok (1996)
17E (8-17 variant)	nlG	50	Zn^{2+}	1.35	10^8	Li et al. (2000a)
39E	alG.	50	UO_2^{2+}	1.0		Liu et al. (2007)
10-23	rly	50	Mg^{2+}	10	10^5	Santoro and Joyce (1997)
8-17	alg	50	Mg^{2+}	10		Santoro and Joyce (1997)
Bipartite	ala	40	Mn^{2+}	1.6		Feldman and Sen (2001)
8-17-like[b]	nlN	various	Mg^{2+}+Mn^{2+}	0.001 to 10		Cruz et al. (2004)

[a]Lowercase letters denote ribonucleotides, uppercase letters are used for DNA nucleotides; bold font: deoxyribozymes that cleave all-RNA substrates
[b]8-17 variants are known for all 16 possible dinucleotide junctions
n.k. = not known (not reported)

The most prominent and most widely studied classes of RNA-cleaving deoxyribozymes are the 10-23 and 8-17 DNA catalysts (Fig. 2b, c), which were first reported in 1997 (Santoro and Joyce 1997). A large variety of other RNA-cleaving DNA catalysts has been isolated by in vitro selection under various conditions, including specific metal ions or pH conditions. For example, DNA enzymes have been characterized that cleave (fluorophore-labeled) chimeric RNA–DNA substrates under acidic conditions, ranging from pH 3 to pH 6 (Liu et al. 2003). Others have been selected for the specific detection of uranium as uranyl ions UO_2^{2+} (Liu et al. 2007). An interesting RNA-cleaving deoxyribozyme has been generated from a binary nucleotide alphabet, which contains only guanosine and cytosine nucleotides, and still exhibits considerable Mn^{2+}-dependent cleavage activity (Schlosser and Li 2009b). An overview on selected examples of RNA-cleaving DNA enzymes and respective references can be found in Table 1. Excellent reviews are available that describe the details of in vitro selection and characterization of these DNA catalysts (Silverman 2005; Baum and Silverman 2008; Schlosser and Li 2010). In the following section, we focus on 10-23 and 8-17 DNA enzymes since most preclinical studies on DNA catalysts as therapeutic agents have been conducted with 10-23 deoxyribozymes, and 8-17 variants have found wide applications as components of biosensors.

4 On Mechanism and Folding of 10-23 and 8-17 Deoxyribozymes

The deoxyribozymes 10-23 and 8-17 were identified by in vitro selection with the goal to find general RNA-cleaving DNA catalysts that function under conditions resembling physiological environment (Santoro and Joyce 1997). The names are rather arbitrary and reflect the selection round and the clone number of the identified DNA. Both DNA enzymes turned out as useful catalysts to cleave all-RNA substrates with practically useful rate constants, ranging from 0.1 min^{-1} under simulated physiological conditions (2 mM Mg^{2+}) and up to 10 min^{-1} in the presence of high divalent metal ion concentrations (100 mM Mg^{2+}). Although the DNA enzymes have been biochemically characterized (Santoro and Joyce 1998), the exact catalytic mechanism of RNA cleavage is not yet understood in detail. Currently, no structure of a deoxyribozyme in an active conformation is known. A small number of reports describe attempts to solve the X-ray crystal structure of the10-23 DNA in complex with an uncleavable substrate (Nowakowski et al. 1999). However, the crystals revealed a dimeric DNA structure in an unproductive conformation that resembled a Holliday junction structure. A preliminary report on NMR structural studies confirmed secondary structure formation between substrate and deoxyribozyme, but no follow-up studies on more detailed NMR structural data have yet been reported (Choi et al. 2000). Below we summarize the reported results from biochemical and biophysical investigations on 10-23 and give a short overview on selected data on DNA folding studies of 8-17 deoxyribozymes [a recent comprehensive review on 8-17 DNA enzymes can be found in (Schlosser and Li 2010)].

4.1 The 10-23 Deoxyribozyme

The 10-23 deoxyribozyme generally cleaves an RNA substrate between a purine and a pyrimidine nucleotide (see Fig. 2b) and is active in the presence of Mg^{2+}, Mn^{2+}, or Ca^{2+} as divalent metal ion cofactor (Santoro and Joyce 1998). A linear increase in k_{obs} with a slope close to 1 was observed between pH 6.5 and 8.5, indicating that a single deprotonation event is part of the rate-determining step of RNA cleavage. Most likely, this reflects deprotonation of the 2′-OH group at the cleavage site, but it is not known if any of the core nucleotides could act as a general base to assists the deprotonation. In order to identify functionally relevant nucleotides in the catalytic core of the 10-23 DNA catalyst, a comprehensive mutation analysis was performed (Zaborowska et al. 2002). All 15 nt in the catalytic core were individually replaced by each of the other three natural nucleotides. The activity of the 45 mutants was evaluated by single time-point measurements of the cleaved RNA fraction under single turnover conditions (37°C, 20 min, in 50 mM Tris pH 7.5, 10 mM Mg^{2+}). Selected mutants were used for full kinetic measurements of k_{obs}. A number of

Table 2 Effects on catalytic activity of mutations and modifications in the catalytic core of the 10-23 deoxyribozyme

nt	G	G	C	T	A	G	C	T	A	C	A	A	C	G	A
Position	1	2	3	4	5	6	7	8	9	10	11	12	13	14	15
Mutation															
G			×	×	×		~	√	~	√	√	~	×		√
A	×	×	√	×		×	√	√		√			~	×	
C	×	×		×	√	×		√	×		~	√		×	×
T	×	×	~		×	×	√		√	√	√	√	×	×	~
Modification															
Inosine (I)	~	~	×	×	×	√	×	√	~	√	√	√	×	×	√
Purine (P)					√										
2AP						×								×	
c^7A					×						×	~			√
c^7G						×									
Deletion	×	×	×	×	×	×	√	√	~	×	~	×	×	×	×
Abasic	√	~	√	×	×	×	×	√	×	×	~	~	×	×	×
C3 linker	√	~	~	×			×		×	×	×	×			×
2′OMe	×	√	×	×	×	×	√	√	~	×	√	~	×	√	√
2′(*R*)CH_3				×				×							
2′(*S*)CH_3				×				√							
LNA				√				×							
PS	+	~	√	~	×	√	√	+	~	~	~	~	~	√	√

√ = modification is tolerated (no effect on catalytic activity), + = modification enhances catalysis, ~ = slightly reduced catalytic activity (less than 50% change in k_{obs} or final yield), × = modification is detrimental [no activity or trace amount of cleavage product (<10% of wt)]; empty fields indicate that this modification was not investigated on this position. For abbreviations and nucleotide structures see Fig. 3 and Fig. 4

nucleotides were found to be important (summarized in Table 2): nucleotides G1, G2, T4, G6, and G14 could not be replaced by any other nucleotide without complete loss of catalytic activity. In contrast, nucleotides at positions 7–12 could mostly be exchanged to any other of the natural nucleotides. In addition, the exocyclic functional groups of certain nucleotides were investigated. For example, inosine (Fig. 3) was comprehensively tested at all positions, and interesting results were found at positions C3 and C13. Based on the striking difference of adenosine and inosine substitution (adenosines were partially tolerated in place of cytidines, but inosines were detrimental), it was speculated that an exocyclic amino group is essential (originating from C or A). For position G6, the O^6-carbonyl group was found to be the most important feature because activity was abolished with adenine, but inosine did not have any effect. At position G14, both the N^2-amino and the O^6-carbonyl groups were essential, as indicated by the intolerance for inosine and 2-aminopurine. Interestingly, at position A5, cytidine showed some activity, but inosine was detrimental, again pointing toward an important amino group. However, when A5 was changed to purine, no change in activity was observed, indicating that another functional group must be responsible for the observed effects. It was speculated that a likely candidate is the lone pair of the N^1 ring nitrogen of adenine, which is also

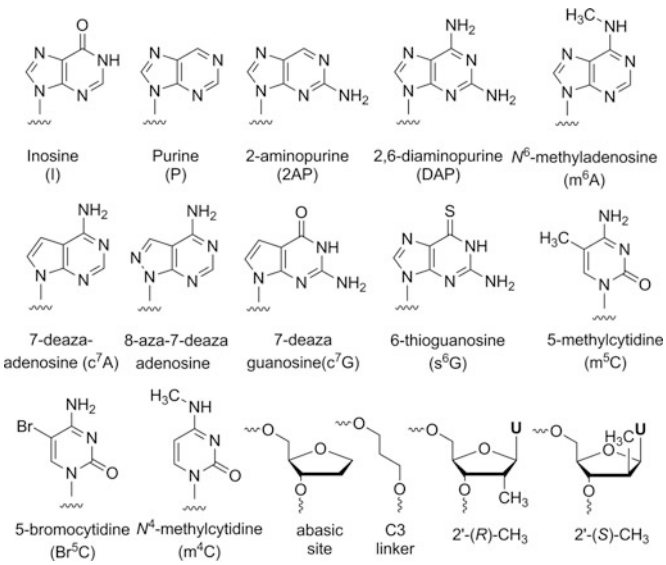

Fig. 3 Nucleoside modifications used to study mechanistic aspects of 10-23 and 8-17 deoxyribozymes (see also Fig. 4 for more examples)

found in purine, and analogously at N^3 of cytosine, but not in inosine and guanosine, which carry a protonated NH group as part of the lactam functionality. However, in a recent study, it was shown that c^7A (Fig. 3) at position A5 was detrimental, clearly pointing toward the importance of the N^7 atom (He et al. 2011). Interestingly, the activity of 10-23 was rescued by placing a nitrogen atom at position 8 of the purine ring, i.e., 8-aza-7-deaza-deoxyadenosine at position A5 supported phosphodiester cleavage. A similar effect was observed at position A11.

The mutation data revealed considerable flexibility at positions 7–12 but also suggested conserved nucleotides that are likely involved in formation of the catalytic structure. These results should prove helpful for interpretation of high-resolution deoxyribozyme structures; unfortunately, such structural data remained elusive up until today. Nevertheless, the mutation analysis highlighted essential nucleotides, and the results also give information on which positions might be amenable to chemical modifications or functionalization to protect the core against endonucleolytic attack or to modulate enzymatic activity.

The traditional enzymology approach, as described above, provides highly valuable data, but the process is rather laborious and time-consuming. Recently, combinatorial methods have been developed for the simultaneous assessment of all nucleotides in the catalytic core of DNA enzymes. Combinatorial mutation interference analysis (Wachowius et al. 2010) and nucleotide analog interference mapping of DNA (Wachowius and Höbartner 2011) were also applied to 10-23 and efficiently revealed essential residues that are largely comparable to the results from individual mutants (C. Höbartner, F. Wachowius, unpublished results).

To further narrow down the features of the catalyst, another study addressed the deletion of individual nucleotides from the 10-23 core (Zaborowska et al. 2005). It was found that C7 and T8 can be separately removed without severely affecting cleavage activity, but other tested deletions were detrimental. The double deletion of C7 and T8 resulted in about twofold reduced k_{obs} compared to the unmodified DNA, but the shortened deoxyribozyme was not able to cleave long RNA substrates. The effect of deleting individual nucleobases (instead of entire nucleotides) was systematically examined by replacing every nucleotide with an abasic site analog (a tetrahydrofuran derivative, Fig. 3 (Wang et al. 2010). Additionally, every nucleotide was replaced by an acyclic C3 linker (Fig. 3), which keeps the same number of atoms in the backbone chain, but confers much increased conformational flexibility to the DNA chain. The results from this study corroborated earlier findings on nucleotide requirements in the catalytic core and, in addition, defined the importance of structural preorganization of the DNA backbone by certain 2′-deoxyribose units. It is interesting to point out that substitution of T8 with an abasic site or the acyclic linker resulted in slightly increased deoxyribozyme activity compared to the parent DNA, whereas deletion of the entire nucleotide resulted in about twofold reduced k_{obs}. However, it should be noted that the activity tests (Wang et al. 2010) were done with a substrate containing a single embedded ribonucleotide, as opposed to the full RNA substrate used in the deletion and mutation analyses (Zaborowska et al. 2005).

In an earlier study, a 10-23 mutant was identified, which was 4 nt shorter than the parent DNA, and which showed high activity in the presence of Ca^{2+}, but had very low activity in the presence of Mg^{2+} (Sugimoto et al. 1999). A functional group mutation analysis in this variant identified the importance of carbonyl groups at G1 and G2 and showed that A7 and A8 could not be replaced by 2,6-diaminopurine (Fig. 3). These detrimental modifications affected the K_m, but did not influence k_{cat}; only one mutation, namely, G10-2AP, dramatically affected the k_{cat}. Moreover, 5-propinyl-C increased the catalytic activity by decreasing K_m (ca. fivefold) and increasing k_{cat} (almost twofold).

The tolerance of the 10-23 core nucleotides to ribose modifications was also investigated. In a comprehensive study reported in 2003, all loop nucleotides were systematically replaced by their 2′-OMe counterparts (Schubert et al. 2003). The activity assay revealed that the 2′-OMe group was detrimental at 9 out of 15 loop positions. When the remaining 6 nt simultaneously contained the 2′-OMe modification, the k_{obs} dropped by only twofold. A detailed discussion on the effect of 2′-OMe modifications can be found in Sect. 5.2. More recently, the influence of 2′-C-methyl modified uridine nucleotides (Fig. 3) at positions 4 and 8 of the 10-23 core sequence was investigated (Robaldo et al. 2010). The absolute configuration of the methyl group had a pronounced effect on the catalytic activity. This observation is most likely related to the different preferred sugar pucker conformations of 2′-(R)- and 2′-(S)-CH_3 modified nucleosides. Interestingly, incorporation of the 2′-(S)-CH_3 derivative at position 8 had little effect, whereas the 2′-(R)-CH_3 derivative reduced the cleavage rate by tenfold, at different Mg^{2+} concentrations between 0.5 and 10 mM. This is interesting with respect to the above-mentioned finding that

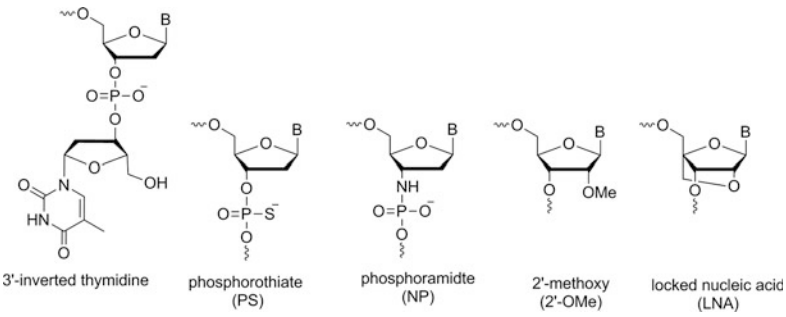

Fig. 4 Chemical modifications that have been introduced in RNA-cleaving DNA enzymes to impart drug-like properties

nucleotide T8 can be deleted without significantly affecting DNA activity. Introducing the modification at position 4 resulted in mostly inactive DNA variants at low Mg^{2+} concentrations. This 2′-C-methyl ribose modification is also appealing with respect to increased nuclease resistance of the modified DNA. Along the same lines, it should be mentioned that LNA nucleotides (Fig. 4) were tested at positions T4 and T8 in the catalytic core of the deoxyribozyme (Robaldo et al. 2010). Although LNA-T was more or less tolerated at T4, the T8-modified and double-modified derivatives exhibited drastically reduced catalytic activity, again indicating sensitivity to local structural changes induced by the conformationally restricted nucleotides. In contrast, LNA and 2′-OMe modifications were shown to be beneficial when introduced into the binding arms of 10-23 deoxyribozymes (Schubert et al. 2003; Donini et al. 2007). This will be discussed in more detail in the context of potential therapeutic applications in Sect. 5.

Besides nucleobases, the phosphate backbone can also be involved in the catalytic mechanism or in coordination of metal ions. Therefore, it is important to investigate functional and essential phosphate groups in the deoxyribozyme core region. In this respect, one nonbridging phosphate oxygen was systematically replaced by sulfur at every internucleotide phosphodiester bond of 10-23 (Nawrot et al. 2007). The cleavage kinetics were investigated in the presence of Mg^{2+} and of Mn^{2+}, in order to analyze the "thio" and "rescue" effects, following the hard and soft acids and bases (HSAB) principle. In the presence of Mg^{2+}, a 16-fold reduction in k_{obs} was observed when the phosphorothioate (PS) modification was placed at A5. This derivative also showed the largest rescue effect with Mn^{2+} ($k_{obs}Mn/k_{obs}Mg = 176$). By a combination with 6-thioguanosine substitution at position G6, it was suggested that a likely metal ion binding site is formed involving the carbonyl group of G6 and the phosphodiester between T4 and A5. Additional indication for a potential metal ion interaction was observed for the phosphodiester between T8 and A9. At nucleotides 3, 6, 7, and 14 of the loop, the sulfur substitution was well tolerated, and at nucleotides 1 and 8, the phosphorothioate even enhanced catalytic activity. It should also be noted as an advantage that the phosphorothioate modification confers increased nuclease stability to the DNA. Improved activity combined with increased

stability provides interesting opportunities for biological or therapeutic applications (see also Sect. 5). In addition, the effect of phosphorothioate substitution at the scissile phosphate in the RNA substrate was investigated. Differential effects were found for the activity of 10-23 upon interaction with R_p- and S_p-phosphorothioate-containing substrates (Nawrot et al. 2008; He et al. 2002). While the S_p thio analog was efficiently cleaved with only slightly reduced rates compared to the unmodified RNA substrate, the R_p-configured phosphorothioate was resistant to cleavage by 10-23, even at high Mg^{2+} concentrations (up to 100 mM). Interestingly, this severe thio effect could not be rescued by the more thiophilic Mn^{2+} ions. These results suggest that the nonbridging oxygen atoms at the scissile phosphodiester bond are most likely not directly coordinated to metal ions, thus indicating that the catalytic mechanism does not involve metal-mediated charge neutralization at the nonbridging oxygen atoms. Rather, it is likely that metal ions directly coordinate to the 2′ oxygen and 5′ oxygen, facilitating deprotonation of the attacking 2′-OH group and neutralization of the developing charge at the 5′-phosphate terminus. Furthermore, it was hypothesized that the proton of the 2′-OH group migrates to the pro-R_p oxygen of the phosphate. This is consistent with the inactive nature of the R_p(S) substrate since the lower pK_A of the phosphorothioate compared to an unmodified phosphate would render H-migration less plausible. Further studies are expected in the near future, taking advantage of recently reported methods to produce 3′- and 5′-phosphorothiolate substrates, that could be helpful for disentangling the metal ion contributions to DNA-catalyzed RNA cleavage, similar to strategies employed for the investigation of ribozyme catalysis (Frederiksen and Piccirilli 2009).

Although there are some striking similarities between DNA-catalyzed RNA cleavage and hammerhead ribozyme activity, some experimental results do not fit into the picture of superimposable mechanisms. For example, the behavior of hammerhead and 10-23 against trivalent lanthanide ions is different. While the hammerhead ribozyme gives a bell-shaped curve of activity versus increasing La^{3+}-concentrations (in a background of constant Mg^{2+} concentration, i.e., activation at low [La^{3+}] and inhibition at high [La^{3+}]), the 10-23 DNA enzyme shows gradual inhibition (investigated between 0.5 and 10 μM $LaCl_3$) (He et al. 2002). Lanthanide probes were also used for studying the RNA cleavage by a Pb^{2+}-dependent deoxyribozyme (Geyer and Sen 1998), which was found to tolerate lanthanide ions for phosphodiester cleavage. A single lanthanide ion was most likely directly interacting with the 2′-OH group at the cleavage site. Different lanthanides were tested, showing that the smaller lanthanides (Tb^{3+}, Tm^{3+}, Lu^{3+}) more efficiently supported DNA-catalyzed phosphodiester cleavage compared to larger ones (Eu^{3+}, Nd^{3+}, Ce^{3+}, La^{3+}). These results were corroborated by Tb^{3+} luminescence experiments involving unmodified and phosphorothioate-containing substrates, which showed that the 2′-OH group was required for efficient Tb^{3+} binding, but the phosphate backbone at the cleavage site was likely not involved in direct metal ion contacts (Geyer and Sen 1998). Tb^{3+}-luminescence spectroscopy was used in a similar way to investigate metal ion binding in 8-17 deoxyribozymes [see Sect. 4.2; (Kim et al. 2008)].

Metal ions not only play a mechanistic role for DNA catalysis but probably possess an equally important structural role. By neutralizing negative charges, coordinating to phosphate groups and nucleobases, metal ions can induce proper folding of the DNA into a catalytically active conformation. Structural rearrangements upon metal ion binding were studied in the 10-23 DNA enzyme by fluorescence resonance energy transfer between two fluorophores, rhodamine and fluorescein, attached at the 5′- and 3′-termini of the binding arms (Cieslak et al. 2003). Fluorescence anisotropy experiments at different Mg^{2+} concentrations were also reported. The results showed that structural transitions in the DNA enzyme leading to a decreased end-to-end distance of the fluorophores occur at rather low Mg^{2+} concentrations, at which the deoxyribozyme does not yet have full activity (i.e., the folding midpoint observed by FRET was at ~2 mM Mg^{2+}). Since higher Mg^{2+} resulted in improved cleavage activity, but no further reduction of the FRET distances was observed, it was suggested that structural transitions at low Mg^{2+} concentrations are not sufficient for optimal catalytic activity. However, it is also conceivable that the single combination of fluorophores at terminal positions might not be ideal to observe subtle conformational changes required for activity. In this respect, more detailed studies (including single-molecule fluorescence experiments) were carried out for 8-17 deoxyribozymes, as discussed in Sect. 4.2 (Kim et al. 2007b; Lee et al. 2007, 2010).

As mentioned above, no 3D structure of 10-23 is available in an active conformation that would facilitate elucidation of structure–function relationships. Although a large amount of biochemical and biophysical data are available from the above-described reports, the relationship between tertiary structure and function remains unknown. Recently, a preliminary model for the tertiary structure of the 10-23 deoxyribozyme was investigated in silico using coarse-grained Brownian dynamics simulations (Kenward and Dorfman 2009). It was found that the DNA enzyme bends its substrate away from the cleavage point and a transition state was suggested with a buckled catalytic core. After the cleavage, a substantial extension of the end-to-end distance of the binding arms was observed. It is expected that this model provides the starting point for more detailed molecular dynamics simulations of deoxyribozymes and will be helpful to draw connections from experimental data to computational results.

4.2 The 8-17 Family of Deoxyribozymes

The “original” 8-17 deoxyribozyme (Fig. 2c) has a preference for cleavage of RNA substrates between adenosine and guanosine (Santoro and Joyce 1997). The catalytic core consists of 13–15 nt that present a typical 3-bp stem and a 3-nt loop as the characteristic features. Interestingly, this motif has been isolated more than five times from independent in vitro selection experiments in different laboratories (Li et al. 2000a; Peracchi 2000; Cruz et al. 2004; Schlosser et al. 2008a). The recurrence of this small motif makes it an interesting subject for fundamental studies on DNA catalysis but also has a practical benefit as a small, cheap, stable, and versatile

endoribonuclease. Interestingly, out of the 15 nt organized into a defined three-way junction secondary structure, only 4 nt are absolutely conserved in more than 150 in vitro selected 8-17-like deoxyribozymes (Cruz et al. 2004). These are confined to A6, G7, C13, and G14 (underlined in Fig. 2c). Using deoxyribozyme analogs with modified nucleotides, the functional groups of these 4 nt essential for catalytic activity have been identified (Peracchi et al. 2005). It was found that A6 and G7 are sensitive to sterically demanding substitutions since m^6A (Fig. 3) had a larger impact on catalysis than purine at position A6, and s^6G supported catalysis even less efficiently than 2-aminopurine at position G7, which slowed down the reaction by about 1,000-fold. These results suggested the presence of a functionally important hydrogen-bonding network involving various H-bonding donors and acceptors of these two purine nucleotides. The most critical functional group of G14 was found to be the exocyclic amino group. Interestingly, s^6G (Fig. 3) was well tolerated under standard reaction conditions, but activity was strongly inhibited by submillimolar concentrations of thiophilic Cd^{2+} ions. This suggested that a strong direct metal coordination at this functional group does not support catalysis. On the contrary, the nucleotide at position 12 was found to modulate the metal ion cofactor requirements. While 8-17 with thymidine at position 12 is active with Mg^{2+}, Mn^{2+}, and Ca^{2+} to similar extents, a DNA enzyme with inosine at position 12 used Ca^{2+} fivefold more efficiently than the parent enzyme (activity with Mg^{2+} and Mn^{2+} was even slightly inhibited by the inosine mutation). Although such interesting observations cannot directly prove the participation of individual functional groups in the catalytic mechanism, they provide useful insights into potential tertiary interactions and may suggest structure–function relationships that can help model building and engineering of modified deoxyribozymes.

Sequence variations beyond these four conserved nucleotides were found to influence the efficiency of substrate cleavage and the nucleotide requirements and tolerance at the dinucleotide cleavage site (Schlosser et al. 2008b). Systematic characterization identified a subset of optimal 8-17 variants that can cleave all 16 possible dinucleotide junctions in chimeric RNA–DNA substrates (containing a single ribonucleotide). However, only a subset of dinucleotide junctions is efficiently cleaved in all-RNA substrates (Silverman and Baum 2009; Schlosser and Li 2010).

A variety of other biophysical studies have been conducted to collect insights into how individual residues contribute to folding and catalysis of 8-17 deoxyribozymes using different metal ion cofactors, including Mg^{2+}, Zn^{2+}, and Pb^{2+}. Metal-dependent folding of the 8-17 DNA enzyme was studied by bulk and single-molecule FRET experiments. The bulk study used a fluorophore-labeled DNA enzyme in complex with an inactivated substrate, in which the ribonucleotide at the cleavage site was replaced by a deoxyribonucleotide (Kim et al. 2007a). The DNA enzyme was found to fold into a pyramidal structure in the presence of Mg^{2+} and Zn^{2+}, but with Pb^{2+}, no global folding transition was observed (although Pb^{2+} is the most effective cofactor). A recent three-color bulk FRET study tried to correlate the metal-dependent folding with the identity of the dinucleotide junction in the

substrate (Lam and Li 2010). It was found that DNA enzyme–substrate complexes with purine–purine junctions folded at lower Mn^{2+} concentrations than those containing pyrimidine–pyrimidine junctions, which is consistent with cleavage activity studies. Nevertheless, bulk studies with inactive substrates may be suboptimal to support strong conclusions on folding transitions. To exclude adverse effects of the inactive substrates which might change metal-binding properties, single-molecule FRET experiments were carried out which allow individual active deoxyribozymes to be studied with cleavable substrates. Moreover, smFRET can detect and distinguish less populated conformations that may be important for activity but that cannot be resolved in bulk FRET measurements. Using a total internal reflection (TIR) fluorescence microscope to observe fluorescently labeled, surface-bound deoxyribozymes, two distinct folding pathways that depend on the identity of the metal ion cofactor were confirmed (Kim et al. 2007b). In the presence of Mg^{2+} and Zn^{2+}, a structural change occurs before the cleavage step. In contrast, Pb^{2+} is accommodated in a prearranged conformation of the deoxyribozyme which directly leads to RNA cleavage. In another report, three-color alternating-laser excitation (3c-ALEX) was used to study the branched structure of 8-17 at the single-molecule level in solution (Lee et al. 2007). Again, different metal ion conditions resulted in different folding pathways of the DNA. Moreover, the important roles of A6 and G7 were confirmed, and it was shown that they are functionally involved in productive folding into an active conformation. Single-molecule experiments using ALEX-FRET were also demonstrated to provide accurate measurements of the cleavage rate of 8-17 deoxyribozymes and allowed the determination of apparent metal ion binding constants (Lee et al. 2010).

Metal ion binding in the 8-17 deoxyribozyme was also investigated by Tb^{3+} luminescence spectroscopy (Kim et al. 2008). These studies rely on the sensitized luminescence of Tb^{3+} by energy transfer from nucleic acids which can be detected at 543 nm. Tb^{3+} was found to reversibly inhibit 8-17 activity by competing for binding sites that are productively occupied by effective metal ion cofactors. Again, different effects were observed for Zn^{2+} and Pb^{2+}, and it was concluded that Pb^{2+} may bind to a different site than Zn^{2+} or Mg^{2+}. The differences in local and global folding induced by various metal ions were also studied by contact photo-cross-linking experiments using photoactivatable nucleotide analogs (Liu and Sen 2008, 2010). In particular, s^6G (Fig. 3) was incorporated into the substrate at the cleavage site and separately at various positions in the catalytic core. The thionucleotide in the enzyme substrate complex was excited by irradiation with UV light, and the cross-linked positions were identified by a combination of piperidine cleavage and primer extension experiments. These cross-linking studies resulted in a model for the active structure of the deoxyribozyme, in which the functionally essential nucleotides of the catalytic core, in particular G7 and G14, enclose the cleavage site in a sandwich-like topology (Liu and Sen 2008). Moreover, the results corroborated distinct properties of Pb^{2+}-activated deoxyribozymes, with respect to local conformation changes as opposed to global folding of the DNA enzyme–substrate complex (Liu and Sen 2010).

5 Potential Therapeutic Applications of RNA-Cleaving Deoxyribozymes Against Bacteria and Viruses

Ever since the discovery of RNA-cleaving 10-23 and 8-17 DNA enzymes, attempts have been embarked to exploit them as therapeutic agents by utilizing their ability to cleave disease-related mRNAs. Compared to other oligonucleotide-based gene silencing strategies, DNA enzymes offer several advantages (Bhindi et al. 2007). First of all, DNA enzymes do not require any cellular enzymes like RNase H (as for antisense strategies) or argonaute 2 (as for RNAi) to exhibit their cleavage activity on target RNAs. Compared to ribozymes, DNA enzymes are more target specific, and due to their versatility in target cleavage, identification of potential targets is relatively easy. Moreover, DNA is cheap and easy to synthesize compared to siRNAs or ribozymes. However, similar to other antisense technologies, the therapeutic utility of DNA enzyme is hampered by the present lack of efficient delivery agents. Therefore, although a plethora of reports is available in the literature on the use of DNA enzymes in in vitro settings and in animal models (Dass et al. 2008; Benson et al. 2008; Peracchi 2004), no clinical trials have so far been reported for an RNA-cleaving DNA enzyme. The therapeutic targets of RNA-cleaving DNA enzymes can be broadly classified into cancer, cardiovascular, allergy-related, bacterial, and viral targets. A detailed discussion on the DNA enzyme-mediated attenuation of all these targets is beyond the scope of this chapter. For a comprehensive outlook, readers are directed to the recent reviews available in the literature (Bhindi et al. 2007; Dass et al. 2008; Benson et al. 2008; Peracchi 2004; Achenbach et al. 2004). Here we focus on DNA enzyme-based strategies against bacteria and viruses. The therapeutic targets covered in this section and the observed effects of deoxyribozyme action are summarized in Table 3.

5.1 DNA Enzymes Targeting Bacteria

The utility of 10-23 DNA enzymes to cleave the mRNA of isocitrate lyase (*ICL*) of *Mycobacterium tuberculosis* has been investigated (Li et al. 2005). ICL is an enzyme which plays an important role in the metabolism of *M. tuberculosis* in the latent state of infection in macrophages. Therefore, *ICL* is one of the emerging targets for antituberculosis therapy. In vitro cleavage assays on a 1,871-nt-long ICL transcript in the presence of 15 mM Mg^{2+} (50 mM Tris–HCl, pH 7.0 at 37°C) revealed modest target attenuation by four out of five DNA enzymes tested. Under the same conditions, an analogous enzyme bearing mutations in the catalytic core was completely inactive. The DNA enzymes were tested to evaluate their ability to suppress the expression of *ICL* and thereby reduce the survival of *M. tuberculosis* in THP-1 cells. Since DNA enzymes were not capable of penetrating the cell wall of *M. tuberculosis*, suboptimal concentration of the antituberculosis drug isoniazid (INH) was used to soften the cell wall. After 4 and 7 days of treatment with DNA

Table 3 Targets and effects of antibacterial and antiviral RNA-cleaving deoxyribozymes

Disease/target	Strain/cell/ animal/RNA	DNA enzyme/ modification	Efficiency	References
Bacterial targets				
M. tuberculosis (*ICL*)	THP-1 cells	10-23	55–60% Growth reduction	Li et al. (2005)
M. tuberculosis (*TACO*)	RAW264.7 cells	10-23 (expr. vector)	78% Reduction in mRNA and 75% reduction in protein levels	Li et al. (2010)
ftsZ	DH5αpro cells	10-23 (expr. vector)	55–65% Growth reduction	Tan et al. (2004)
β-Lactamase	TEM-1 and TEM-3 strains	10-23 (and expr. vector)	58–63% Growth reduction (electroporated); 46–71% (vector based)	Chen et al. (2004a, b)
Methicillin-resistant *Staphylococcus aureus* (*blaR1*)	WHO-2 strain	10-23 (PS-mod.)	62% Reduction in colonies and 70% reduction in mRNA	Hou et al. (2007)
Viral targets				
HIV				
CCR5 and CXCR-4	HeLa and U87 cells	10-23	Inhibition of cell membrane fusion (based on luciferase reporter assay)	Goila and Banerjea (1998), Basu et al. (2000)
V3 loop	U87.CD4.CXCR4 and U87.CD4.CCR5 cells	10-23	68–81% of inhibition of viral replication	Zhang et al. (1999)
GAG	COS-1 cells	10-23	10-fold reduction of mRNA levels ; 95% reduction of HIV-1 gene expression (luciferase reporter assay)	Sriram and Banerjea (2000), Dash and Banerjea (2004), Sood et al. (2007a)
TAT and *TAT/REV*	THP-1 cells	10-23	8–10-fold reduction of mRNA levels	Unwalla and Banerjea (2001a, b), Sood et al. (2007b), Unwalla et al. (2006)
TAR	HeLa cells	10-23	80% Reduction of HIV indicator p24 antigen	Chakraborti and Banerjea (2003)
VPR-B, VPR-C	293-T cells	10-23	3.5- to 5-fold reduction of mRNA levels	Bano et al. (2007)
DIS and PBS at the 5′-UTR	HEK 293-T cells	10-23 (LNA mod.)	100% Reduction of viral antigen CA-p24	Jakobsen et al. (2007), Vester et al. (2006)

Hepatitis B and C				
5′-NCR	Huh7 cells	10-23 (PS-mod.)	45–67% Reduction of RNA (luciferase reporter assay)	Oketani et al. (1999)
5′-UTR	293rTA and Huh7 cells	10-23 (PS-mod.)	24–48% Reduction of viral RNA	Trepanier et al. (2006)
HCV 1b RNA	Huh7 cells	10-23 (2′-OMe mod.)	61% Reduction of viral RNA and 59% reduction of viral protein	Trepanier et al. (2008)
5′-UTR of IRES	Huh 7 cells	10-23	81% Inhibition of gene translation (luciferase reporter assay)	Roy et al. (2008)
X gene	HepG2 cells	10-23	4–6-fold reduction in X protein	Goila and Banerjea (2001)
X gene	AD293 cells	10-23	60% Reduction of protein, 80% reduction of RNA (GFP reporter assay)	Hou et al. (2006)
Other viral targets				
E6/*E7* (HPV)	SiHa cells	10-23 (2′-OMe /LNA mod.)	50% Reduction of RNA	Reyes-Gutierrez and Alvarez-Salas (2009)
E6/*E7* (HPV)	830-nt E6/E7 transcript (*in vitro*)	8-17 (LNA mod.)	$k_{obs} = 0.025–0.044\ min^{-1}$	Donini et al. (2007)
F gene (RSV)	Hep-2 cells and RSV-infected mice	10-23 (PS mod.)	Cells: 100% reduction of RNA; 87% reduction of protein; mice: 54% reduction of RNA	Xie et al. (2006), Yang et al. (2007)
3′-NCR (JEV)	J744E cells and JEV-infected mice	10-23 (PS/2′-OMe mod.)	Cells: 108-fold reductions of viral replicationmice: 99.99% inhibition of viral replication	Appaiahgari and Vrati (2007)
TIS (influenza virus A)	MDCK cells	10-23 (N3′-P5′ phosphoramidate linkages at ends)	99% Inhibition of viral replication	Takahashi et al. (2004)
5′-UTR (SARS-CoV)	Vero E6 cells	10-23	55–85% Reduction of protein levels (GFP reporter assay)	Wu et al. (2007)
5′-UTR (HRV-14)	835-nt HRV-14 transcript (in vitro)	10-23 (2′-OMe or LNA mod.)	$k_{obs} = 0.5\ min^{-1}$ and $v_{init} = 4.7\ nM\ min^{-1}$	Schubert et al. (2003)
5′-UTR (CAV-21)	797-nt CAV-21 transcript (in vitro)	10-23 (2′-OMe or LNA mod.)	100% RNA cleavage	Schubert et al. (2004)

expr. expression, *mod.* modification

enzyme at 5 μM concentrations, the bacterial growth (CFU levels) was reduced to 55–60% in comparison with the untreated cells. Since this initial work, no further studies have been reported on *ICL*-targeting DNA enzymes.

Tryptophan–aspartate-containing coat protein (*TACO*) plays a crucial role in the survival of *M. tuberculosis* in macrophages. Recently, researches have reported an efficient way to target this protein by generating 10-23 DNA enzymes in macrophages with the help of a single-stranded DNA expression vector based on Moloney mouse leukemia virus reverse transcriptase (*MMLV-RT*) (Li et al. 2010). To enhance the expression efficiency, the *MMLV-RT* gene and the oligonucleotide sequences for generating the DNA enzymes were cloned into a single plasmid under the control of two separate promoters. The vector was designed to generate the 10-23 DNA enzyme, which targets the coding region of *TACO*-mRNA. Control plasmids expressing mutant enzymes were also constructed. The efficiency of the active DNA containing vector was verified in murine macrophage cell line RAW264.7. Semiquantitative RT-PCR assays revealed a 78% reduction of *TACO*-mRNA levels at 48 h posttransfection. The corresponding reduction of the *TACO*-protein revealed by Western blot was 75%. Mutant plasmids did not induce any reduction of the mRNA or the protein levels. Though these results are encouraging in terms of DNA enzyme delivery, the need to coexpress viral transcriptase might lead to adverse effects. Moreover, the usefulness of this approach to reduce *M. tuberculosis* infection has not yet been reported.

A tetracycline-regulated expression vector based on *MMLV*-RT has been constructed to generate a 10-23 DNA enzyme which is able to target the *ftsZ* gene of bacteria (Tan et al. 2004). The *ftsZ* gene is essential for bacterial cell division and also for cell viability. Therefore, targeting the *ftsZ* mRNA is an attractive way to halt bacterial cell proliferation. When tested in DH5αpro cells, the single-stranded DNA expression vector was not only able to downregulate the *ftsZ* gene expression (revealed by Western blot) but was also able to repress bacterial cell proliferation. This was evident in the reduction (55–65%) of CFU levels and also in the formation of long filamentous cells. The inhibitory effect was found to depend on time as well as the amount of tetracycline used. Unfortunately, in these studies, a control vector expressing a mutant 10-23 enzyme was not investigated, and therefore, the contribution from antisense effect cannot be ruled out.

Targeting genes responsible for antibiotic resistance by RNA-cleaving DNA enzymes is an attractive way to sensitize drug-resistant bacteria to antibiotics. One of the important targets in this class is *β-lactamase* mRNA since *β-lactamase* is responsible for bacterial resistance against β-lactam antibiotics. Two 10-23 DNA enzymes targeting the start codon as well as the coding region of *β-lactamase* mRNA were designed (Chen et al. 2004a). A di-DNA enzyme was also designed by coupling two single DNA enzymes in tandem. In vitro cleavage kinetics using a short RNA substrate in the presence of 10 mM Mg^{2+} (50 mM Tris–HCl, pH 7.6 at 37°C) revealed that the DNA enzyme targeting the coding region had higher catalytic efficiency [$k_{cat}/K_m = 9.1 \times 10^7$ $(mol/L)^{-1}$ min^{-1}] than the enzyme targeting the start codon site [$k_{cat}/K_m = 6.4 \times 10^7$ $(mol/L)^{-1}$ min^{-1}] and the di-DNA enzyme [$k_{cat}/K_m = 3.1 \times 10^7$ $(mol/L)^{-1}$ min^{-1}]. This augmented

catalytic efficiency of the enzyme against the coding region has been attributed to the increase in the target binding affinity (low K_m) due to high GC content in the binding arms. All the DNA enzymes were able to cleave a full-length *β-lactamase* RNA transcript (885 nt) with varying efficiencies (40–70% at 2 h). For in vivo studies, DNA enzymes have been delivered into ampicillin-resistant bacteria (TEM-1 and TEM-3) by electroporation. After 9 h, the growth inhibition assays and the *β-lactamase* activity measurement revealed that the di-DNA enzyme was most efficient in attenuating the drug-resistant mRNA. This is reflected in 58% growth inhibition for TEM-1 bacteria and 63% growth inhibition for TEM-3 bacteria. DNA enzymes bearing mutations in the catalytic core or in the binding arm did not show any activity. This underlines the specificity of the DNA enzyme-mediated approach to silence the *β-lactamase* mRNA. The enhanced in vivo activity of the di-DNA enzyme is intriguing, considering the complex structure of the DNA enzyme due to the presence of multiple catalytic loops and binding arms. To address the limitations of exogenous delivery of DNA enzymes to bacteria, researchers constructed a single-stranded DNA vector to express 10-23 DNA enzymes in vivo (Chen et al. 2004b). Using an M13mp18 phage vector, two circular DNA enzymes which target the same start codon and coding region of *β-lactamase* mRNA were generated. The catalytic efficiency of circular DNA enzymes was reduced to 25–30% of the corresponding linear DNA enzymes. The circular enzymes were shown to replicate inside the TEM-1 and TEM-3 bacteria and also were shown to inhibit bacterial growth. The enzyme targeted to the translation initiation site leads to 46% growth inhibition (53% reduction in *β-lactamase* activity), while the enzyme targeted to the start codon region leads to 71% growth inhibition (67% reduction in β-*lactamase* activity). Though these results are encouraging, the viability of these approaches in macrophages has not been reported so far. The efficient expression of DNA enzyme in such systems will be crucial to the potential success of these approaches in clinical settings.

An RNA-cleaving 10-23 DNA enzyme has also been used to target the *blaR1* gene of methicillin-resistant *Staphylococcus aureus* (MRSA) (Hou et al. 2007). The *blaR1* is involved in the sensor/transducer pathway of *blaR1-blaI-blaZ*, and therefore, targeting *blaR1* can lead to the silencing of *blaZ* gene, which codes for *β-lactamase*. A 10-23 enzyme modified with phosphorothioate linkages (PS) (see Fig. 4) in its binding arms has been introduced into MRSA strain WHO-2 by electroporation. A scrambled oligonucleotide sequence was used as a negative control in these experiments. The DNA enzyme at a concentration of 15 mg L^{-1} was able to reduce the number of WHO-2 colonies to 62% compared to the cells treated with the scrambled control. This leads to partial restoration of antibiotic susceptibility of the bacteria by reducing the minimum inhibitory concentration (MIC) of oxacillin from 32 μg mL^{-1} to 8 μg mL^{-1}. The poor retention of the DNA enzyme in the culture medium was responsible for the insufficient restoration of antibiotic susceptibility. RT-PCR revealed that the attenuation in the *blaR1* and *blaZ* mRNA was 70% and 59%, respectively.

5.2 DNA Enzymes Targeting Viral Diseases

5.2.1 Anti-HIV Strategies

In order to challenge HIV-1 entry and fusion into cells, DNA enzymes have been designed and targeted against the coding region of the chemokine receptor gene CCR5 (HIV coreceptor) (Goila and Banerjea 1998). In vitro cleavage assays on a 1,376-nt-long CCR5 transcript using a 10-23 DNA enzyme having 7-nt binding arms revealed more than 70% cleavage of the target under 2–10 mM Mg^{2+} concentrations. The membrane fusion activity assays using CCR5 reporter in HeLa cells demonstrated the ability of the DNA enzyme to reduce the membrane fusion activity significantly. Control experiments using unrelated DNA enzymes and a 14-mer oligonucleotide lacking the catalytic loop failed to induce any activity. This underlines the specificity of the DNA enzymes against CCR5. In a follow-up study, researchers designed DNA enzymes which target another important chemokine receptor CXCR-4 (Basu et al. 2000). In vitro cleavage assays in the presence of 10 mM Mg^{2+} on a 500-nt transcript revealed excellent cleavage by the DNA enzyme. A di-DNA enzyme in which 10-23 enzymes targeting CXCR-4 and CCR5 are arranged in tandem was able to cleave an engineered RNA target of CXCR-4 and CCR5 with extremely high efficiency. The ability of the CXCR-4 mono- and the di-DNA enzyme to alter the membrane fusion activity has been validated in U87 cells using luciferase-based reporter assays.

10-23 DNA enzymes were employed to target the V3 loop region of the HIV-1 genome (Zhang et al. 1999). Nine different DNA enzymes were tested for cleavage of a 414-nt RNA transcript under single turnover conditions. Four of these enzymes showed >50% cleavage. One enzyme was selected for further evaluation. This DNA enzyme exhibited modest catalytic efficiency [$k_{cat}/K_m = 3 \times 10^3$ $(mol/L)^{-1}$ min^{-1}], which was twofold higher than a ribozyme, targeting the same site. When tested to assess the inhibitory ability toward the replication of HIV-1(NL432) strains in U87.CD4.CXCR4 cells, the enzyme exhibited up to 81% inhibition of viral replication on day 2 of the treatment. However, the inhibitory ability of the enzyme against HIV-1(SF162) strain in U87.CD4.CCR5 cells was up to only 68%. The mutant enzyme, which lacks the catalytic ability, also exhibited 30% inhibition of SF162 replication. This may partially be attributed to the antisense effects of the DNA enzyme, and these results underscore the importance using appropriate control oligonucleotides while studying the DNA enzyme-mediated target cleavage in cellular systems. Single cycle infection assays using a luciferase-based reporter system showed that the DNA enzyme could inhibit the incoming HIV-1 virus to an appreciable extent (up to 74% inhibition after 36 h).

Since the target identification for DNA enzyme-mediated cleavage is challenging, 10-23 DNA enzymes with randomized binding arms (7 nt) were used to find the most efficient enzyme which could cleave the HIV-1 *GAG* RNA (Sriram and Banerjea 2000). Two combinatorial libraries were employed for this target selection approach. One was used to target any AU cleavage site in all AUG codons, and

the other one was designed to target any purine–pyrimidine junction in the HIV 1-*GAG* RNA. After an extensive target screening (10 mM $MgCl_2$ in 50 mM Tris–HCl, pH 8 at 37°C) followed by primer extension analyses, the substrate binding sequences of two enzymes were identified which were able to cleave an AU junction (Dz-1836) and a GC junction (Dz-1810), respectively. However, in vitro cleavage assays using 220-nt transcripts revealed that the activity of both enzymes was suboptimal (<10% cleavage, 10 mM Mg^{2+}). Even under 50 mM Mg^{2+} conditions, the cleavage ability of the Dz1810 was only less than 20%. The cleavage assays using 740-nt-long *GAG* RNA transcript in the presence of 10 mM Mg^{2+} showed improved efficacy for Dz1810, while the Dz-1836 showed complete target cleavage. The RT-PCR analysis 48 h after transfection of COS-1 cells with *GAG* RNA expressing reporter and DNA enzymes revealed that Dz-1836 was able to suppress the *GAG* RNA levels tenfold, while the Dz-1810 enzyme was completely inactive. The anti-HIV activity of the Dz-1836 was further verified in COS-1 cells using a luciferase-based reporter assay in which ~95% reduction in the luciferase activity was observed 48 h after transfection. The specificity of inhibition was supported by testing a mutant enzyme and also an antisense oligonucleotide lacking the catalytic domain of the DNA enzyme. Both control experiments did not show any activity under these conditions. In a follow-up study, researchers investigated the cleavage ability of 10-23 enzymes targeting two different AU cleavage sites of HIV-1 *GAG* (p24) transcript which is 320 nt long (Dash and Banerjea 2004). Both enzymes exhibited different cleavage activities under varying Mg^{2+} concentrations. Though one of the enzymes did not induce any cleavage at 1 mM Mg^{2+}, the second enzyme was able to produce 80% cleavage. These varying cleavage potencies of 10-23 DNA enzymes underscore the importance of target accessibility. It has been recently demonstrated that use of 21-nt antisense oligos targeting both the upstream and downstream regions of DNA enzyme binding sites can dramatically increase the target cleavage (Sood et al. 2007a). Using this approach, a 220-nt HIV-1 Gag transcript was cleaved by 10-23 and 8-17 DNA enzymes which were found to be inefficient without the use of antisense oligos. Though the approach involving antisense oligos to augment DNA enzyme-mediated target cleavage works well in in vitro settings, the viability of such an approach in cellular systems has not been reported so far.

TAT and *REV* are regulatory proteins which play key roles in the transcription and replication of HIV-1. Therefore, targeting these genes provides an attractive way to halt the pathogenicity of HIV. The use of DNA enzymes to cleave *TAT* or *TAT*/*REV* RNAs has been reported (Unwalla and Banerjea 2001b). Several 10-23 enzymes with 7-nt binding arms were designed against the loop regions of *TAT* or *TAT*/*REV* RNA and tested for the cleavage efficiency under different Mg^{2+} concentrations. One 10-23 enzyme was able to cleave a 280-nt *TAT* RNA transcript efficiently in the presence of 1–5 mM Mg^{2+} (50 mM Tris–HCl pH 8 at 37°C). RT-PCR analysis of DNA enzyme-treated COS-1 cells revealed eight- to tenfold reduction in *TAT* expression. The mutant control failed to impart any target reduction, and this supports the specificity of the DNA enzyme-mediated approach to target important genes of HIV-1. It has also been demonstrated that many regions

of *TAT* RNA which are predicted (by secondary structure analysis) to be single stranded are found to be completely inaccessible for DNA enzyme-mediated cleavage. The potency of RNA-cleaving DNA enzyme can also be increased by using them in combination with hammerhead ribozymes (Sood et al. 2007b; Unwalla et al. 2006). A DNA enzyme and a hammerhead ribozyme used in synergy achieved excellent cleavage (60%) of a 107-nt HIV-1 *TAT*/*REV*/*ENV* transcript under physiologically relevant conditions (50 mM Tris–HCl pH 7.5, 150 mM KCl, 1–2 mM $MgCl_2$ at 37°C). *TAT*-specific RT-PCR experiments of DNA enzyme- and ribozyme-treated THP-1 cells have shown 11-fold reduction in the mRNA levels compared to untreated cells. In order to enhance the delivery of 10-23 DNA enzyme to human macrophage cell line THP-1, 10 guanosine residues have been attached at the 3′-end of the DNA enzyme (Unwalla and Banerjea 2001a). A stretch of guanosine residues is known to interact with the scavenger receptor on the cell surface of macrophages (Pearson et al. 1993). In vitro cleavage assays in the presence of 10 mM Mg^{2+} of a 28-nt transcript showed that the guanosine-appended DNA enzymes were able to cleave the target, albeit at a lower efficiency than unmodified DNA enzymes. Cellular uptake assays using fluorescently labeled DNA enzymes demonstrated the ability of guanosine-tailed DNA enzymes to enter cells efficiently without the use of transfection agents. There was eightfold reduction of *TAT* RNA observed in RT-PCR assays, when guanosine-modified DNA enzymes were introduced into cells. This clearly demonstrates the power of guanosine-modified DNA enzymes to inhibit key proteins of HIV-1. Unfortunately, no further studies have been reported using this strategy in order to assess the clinical utility of guanosine tails on DNA enzymes.

The stem region of HIV-1-*TAR* RNA has been targeted using several RNA-cleaving DNA enzymes (Chakraborti and Banerjea 2003). Among the enzymes used, eight had 10-23 catalytic motifs and one contained the 8-17 motif. In vitro cleavage assays revealed that only two 10-23 variants were able to cleave an 80-nt full-length transcript at the single nucleotide bulge in the TAR RNA under 10 mM Mg^{2+} (50 mM Tris–HCl pH 8 at 37°C) conditions. The cleavage efficiency was modest, and it varied from 22% to 31%. A 10-23 mutant enzyme failed to cleave the target. One of the enzymes could induce the target cleavage even in the absence of Mg^{2+} albeit at very low efficiency. Nevertheless, this is one of the few reports of metal ion-independent cleavage by a 10-23 DNA enzyme. The reason for this unprecedented cleavage activity is not clear from the data available in the literature. The authors also demonstrated modest cleavage efficiency of the 10-23 DNA enzymes under simulated physiological conditions (2 mM Mg^{2+}). When both active 10-23 enzymes were cotransfected with the HIV1-encoded DNA into HeLa cells, >80% reduction of HIV indicator p24 antigen was observed. However, the mutant DNA enzyme also led to 40% reduction in p24 antigen which can be attributed to antisense effects. RT-PCR on RNA isolated from DNA enzyme-treated cells indicated 10- to 12-fold reduction in the HIV-1 *TAT* gene expression compared to the control cells which were not treated with DNA enzymes. The mutant DNA enzyme also induced fourfold reductions in *TAT* gene expression. This raises the question on the true catalytic efficiency of the DNA enzymes used in

this study. Further studies on primary cells, human PMBCs, and cell lines infected with HIV-1 demonstrated fourfold reduction in the virus protection compared to the cells treated with mutant DNA enzymes.

Other important HIV-1 targets, which emerged recently for DNA enzyme-mediated gene silencing, are the *VpR*-B and *VpR*-C genes (Bano et al. 2007). *VpR* proteins are known to be responsible for controlling various cellular functions of HIV-1 and the G2 phase cell cycle arrest, thereby contributing to the overall pathology of the virus. In vitro cleavage assays of 315-nt-long *VpR* transcripts in the presence of 10 mM Mg^{2+} (50 mM Tris–HCl pH 8 at 37°C) identified two 10-23 enzymes with 7-nt binding arms which were capable of cleaving both *VpR-B* and *VpR-C* in a highly efficient manner. Mutated DNA enzymes could not impart any target cleavage under these conditions. RT-PCR assays of DNA enzyme-treated 293-T mammalian cells 48 h posttransfection revealed 3.5- to 5-fold reduction of *VpR* RNA. The corresponding reduction in the *VpR* protein was fourfold. It has also been demonstrated that in HeLa-CCR5 cells, the *VpR*-induced G2 cell cycle arrest can be reversed after 48 h by the action of *VpR*-specific DNA enzymes.

The ability of 10-23 DNA enzymes to cleave the 5′-UTR of the HIV-1 genome has been reported (Jakobsen et al. 2007). DNA enzymes having 9-nt binding arms were designed to cleave the accessible regions of the dimer initiation site (DIS) and the primer binding site (PBS) of the 5′-UTR. In vitro single turnover cleavage assays using a 355-nt transcript showed significant target cleavage under 10 mM Mg^{2+} (50 mM Tris–HCl pH 8 at 37°C) conditions. The cleavage efficiency of a DIS-targeting DNA enzyme was augmented to 100% by introducing two LNA (Fig. 4) modifications on each binding arm. It should be noted that the LNA modification could not enhance the cleavage efficiency of an enzyme targeting the PBS site. This underscores the fact that LNA modifications do not always enhance target accessibility and subsequent cleavage, as reported in previous studies (Vester et al. 2006). When tested for the ability to reduce the production of viral antigen CA-p24 in HEK 293-T cells, 72 h posttransfection, both LNA-modified enzymes have shown 100% target downregulation at 20–100 nM deoxyribozyme concentration. However, at these concentrations, significant cytotoxicity was observed. At 4 nM concentrations of DNA enzyme, the target silencing ability of the DIS- and PBS-targeting enzymes was only 3- and 18-fold, respectively.

5.2.2 Anti-hepatitis Virus Strategies

RNA-cleaving DNA enzymes have been utilized to target the hepatitis C virus (HCV) genome in the core and in the 5′-noncoding region (NCR) (Oketani et al. 1999). Under cell-free conditions and in the presence of 10 mM Mg^{2+} (10 mM Tris–HCl pH 7.4 at 37°C), a DNA enzyme having 11-nt binding arms cleaved a 731-nt HCV viral RNA at its core initiation site with high catalytic efficiency [$k_{cat}/K_m = 9.69 \times 10^4$ $(mol/L)^{-1}$ min^{-1}]. Increasing the binding arm length to 15 nt further enhanced the catalytic efficiency about 6.5-fold to [$k_{cat}/K_m = 6.29 \times 10^5$

$(mol/L)^{-1}$ min^{-1}]. The enzyme targeting 5′-NCR was found to be 60-fold less efficient in cleaving the target site than the one targeting core region of HCV RNA. When tested for the target RNA cleavage efficiency using luciferase-based reporter systems in HCV permissive hepatoma Huh7 cells, DNA enzymes modified with phosphorothioate linkages at the 5′- and 3′-ends showed 45–67% silencing of luciferase expression. To distinguish the antisense-mediated silencing of DNA enzymes, mutant enzymes having 15-nt binding arms were used. The results indicated 18–31% reduction of HCV RNA by these enzymes. Based on these results, authors concluded that both antisense and catalytic activities contributed to silencing of the target HCV RNA in cellular systems.

To target highly conserved regions of UTR of HCV, 10-23 DNA enzymes with 15-nt binding arms were modified with two PS linkages at both ends of binding arms (Trepanier et al. 2006). In vitro cleavage studies using a 976-nt-long transcript under 10 mM Mg^{2+} (50 mM Tris–HCl pH 7.5 at 37°C) conditions identified an enzyme with high catalytic efficiency [$k_{cat}/K_m = 5.7 \times 10^4$ $(mol/L)^{-1}$ min^{-1}]. When this enzyme was tested in human epithelial cell line 293rTA and Huh7 cells, the HCV RNA suppression after 24 h was 48% and 24%, respectively, as revealed by RT-PCR. In a follow-up study, researchers used a 10-23 DNA enzyme modified with four 2′-OMe nucleotides at both ends of the binding arms to target conserved regions of HCV 1b RNA (Trepanier et al. 2008). Cell-free cleavage assays using a 976-nt RNA transcript in the presence of 10 mM Mg^{2+} revealed fourfold increase in catalytic efficiency [$k_{cat}/K_m = 2.1 \times 10^5$ $(mol/L)^{-1}$ min^{-1}] compared to PS-modified DNA enzymes targeting the same target site. The RT-qPCR data revealed 61% target silencing in Huh7 cells after 6 h of treatment with the 2′-OMe-modified enzyme. The corresponding reduction of HCV protein was found to be 59% and HCV antigen was 84%. The better performance of 2′-OMe-modified enzyme was attributed to its enhanced target binding affinity.

10-23 DNA enzymes targeting various loop regions of the internal ribosomal entry site (IRES) located in the 5′-UTR of HCV have been reported (Roy et al. 2008). Since IRES RNA is closely associated with translation and viral replication, targeting IRES is an attractive strategy to halt HCV replication. In vitro cleavage assays using a 387-nt HCV-IRES transcript in the presence of 10 mM Mg^{2+} (50 mM Tris–HCl pH 7.5 at 37°C) identified several DNA enzymes with excellent efficiency to cleave IRES RNA of genotype b as well as of conserved sequences belonging to all six genotypes of HCV. A luciferase-based reporter system revealed that only one out of three DNA enzymes against genotype b that were active in vitro was able to inhibit HCV-IRES-mediated translation in Huh7 cells to a substantial level (81%). However, a mutant enzyme failed to show any RNA cleavage. These results were further verified using Northern blot hybridization assays. The ability of DNA enzyme to prevent HCV RNA replication has also been tested in Huh7.5 cells harboring a HCV1b replicon. Semiquantitative RT-PCR results revealed 70% inhibition of HCV1b genotype RNA synthesis by the DNA enzymes.

The versatility of 10-23 DNA enzymes to target the X gene of hepatitis B virus has been reported (Goila and Banerjea 2001). The X gene is a pleiotropic transactivator and augments the expression level of other hepatitis genes.

Two 10-23 DNA enzymes were used to target two highly conserved regions of X gene. A combination of both individual DNA enzymes into a tandem arrangement was also investigated. In vitro cleavage studies using a 465-nt X gene transcript under single turnover conditions at 10 mM of Mg^{2+} (50 mM Tris–HCl, pH 7.5 at 37°C) showed efficient target cleavage (~80% cleavage in 4 h) by the individual DNA enzymes. The cleavage ability of the tandem DNA enzyme was slightly lower (~55% cleavage in 4 h). DNA enzyme mutants failed to show any target cleavage activity. However, at 2 mM Mg^{2+} concentration, the cleavage efficiency was considerably lower for all tested DNA enzymes. The intracellular activity of these DNA enzymes was studied in HepG2 cells. The RT-PCR and Western blot analyses demonstrated more efficient X gene silencing (four- to sixfold reduction of X protein) by the individual DNA enzymes than by the tandem DNA enzyme. In a related study, DNA enzymes targeting the X gene using a HBx-EGFP reporter in AD293 cells have been explored (Hou et al. 2006). Different 10-23 enzymes having binding arms of 7, 8, and 9 nt were used, and their efficiency in target cleavage was monitored by flow cytometry and semiquantitative RT-PCR. Forty-eight hours after transfection, the DNA enzyme-treated cells showed ~60% reduction in fluorescence. The mRNA reduction was found to be ~80%. The control DNA enzymes, which were incapable of cleaving the target RNA, did not show any activity, ruling out antisense effects.

5.2.3 Other Viral RNA Targets

The polycistronic *E6*/*E7* mRNAs of human papillomavirus (HPV) have been an attractive target for nucleic acid-based therapy. The power of 10-23 and 8-17 DNA enzymes to cleave the *E6*/*E7* mRNAs at the bona fide antisense window has been recently demonstrated (Reyes-Gutierrez and Alvarez-Salas 2009). The in vitro cleavage of an mRNA transcript under single turnover conditions revealed that only the 10-23 enzyme was capable of cleaving the target efficiently ($k_{obs} = 0.013$ min^{-1}) compared to the 8-17 enzyme. To enhance the target accessibility and to fine-tune the nuclease stability of 10-23 DNA enzyme, chemical modifications such as PS or 2′-OMe or LNA were introduced at the binding arms and at positions 8 and 12 of the catalytic core. In vitro cleavage assays using a short *E6*/*E7* transcript in the presence of 10 mM Mg^{2+} (50 mM Tris–HCl pH 7.5, 150 mM NaCl, 2 mM spermidine at 37°C) revealed that the PS and 2′-OMe modifications in the catalytic core substantially reduced the cleavage activity compared to unmodified DNA enzymes. The DNA enzymes with 2′-OMe- or LNA-modified binding arms showed enhanced cleavage activity of the target compared to unmodified or PS-modified enzymes. The mutated DNA sequences which served as negative controls did not show any activity which validates the catalytic ability of the 10-23 DNA enzyme sequences. The 2′-OMe- and LNA-modified DNA enzymes were also tested to cleave full-length *E6*/*E7* transcript (>1,000 nt long) under 10 mM Mg^{2+} conditions. In these experiments, only LNA-modified DNA enzyme exhibited target cleavage activity. This can be attributed to the high target binding affinity of LNA-modified

enzymes which help to access the target sites effectively. The LNA-modified DNA enzyme was further evaluated for the target mRNA cleavage in HPV-16-positive tumor cell line SiHa. RT-PCR analysis, 24 h posttransfection, revealed >50% E6/E7 mRNA reduction in cells treated with the LNA-modified DNA enzyme. Moreover, cell proliferation studies revealed dose-dependent killing (>50%) by the LNA-modified DNA enzyme 4 h posttransfection. The true catalytic ability and nontoxicity of LNA-modified DNA enzymes were evident in studies using proper mutant controls as well as in the HPV-16-negative cell line C33-A. This report clearly underscores the potential of LNA-modified 10-23 DNA enzymes to target HPV-16 viral mRNAs. The next logical step will be to test these modified DNA enzymes in mice bearing HPV-16.

In order to decipher the enhanced cleavage efficiency of LNA-modified DNA enzymes targeting long and structured mRNA targets such as E6/E7 mRNA, detailed kinetic and thermodynamic studies have been performed (Donini et al. 2007). In this study, four sets of 8-17 DNA enzymes and corresponding LNA-modified enzymes (4–5 modifications in the binding arms) were designed to target specific AG sites located within the first 200 nt of E6 coding sequence. All these cleavage sites were previously shown to be accessible for ribozyme and DNA enzyme-mediated cleavage. Kinetic studies using a short RNA substrate under single turnover conditions revealed that the LNA-modified DNA enzyme had a similar target association rate constant as the unmodified DNA enzyme. However, the dissociation rate constant of the substrate–enzyme complex was tenfold lower for the LNA-modified variant. Studies on the effect of Mg^{2+} have shown that LNA-modified 8-17 enzyme is capable of cleaving the target efficiently at $\leq$1.5 mM Mg^{2+} (50 mM Pipes-NaOH, pH 7.4 at 37°C) concentration. The enhanced efficiency of the LNA-modified enzyme is attributed to its capability to saturate the substrate at low enzyme concentration (100 nM) due to its high target binding affinity. Cleavage assays using prefolded E6 mRNA transcript (544 nt long) and E6/E7 transcript (830 nt long) have shown that LNA-modified DNA enzymes cleaved the target more efficiently (k_{obs} = 0.025–0.044 min^{-1}) compared to unmodified DNA enzymes (k_{obs} = 0.00007 min^{-1}).

Recently, 10-23 DNA enzymes have been designed to target respiratory syncytial virus (RSV) genomic RNA of subgroups A and B (Xie et al. 2006). In vitro cleavage assays using a 453-nt-long N gene RNA transcript in the presence of 10 mM Mg^{2+} (250 mM Tris–HCl pH 7.4 at 37°C) have shown 68% of the target cleavage after 4 h in a sequence-specific and time-dependent manner. Antisense oligonucleotides and a mutant DNA enzyme targeting the same site failed to produce any cleavage. When the DNA enzyme was tested in RSV-infected Hep-2 cells, 96% protection of RSV-infected cells was obtained after 5 days of treatment. Semiquantitative RT-PCR assays revealed 100% reduction of RSV F mRNA after 3 days of incubation with the DNA enzyme. These results were validated by Western blots in which the reduction of the RSV F protein level was up to 87%. The results obtained from these studies were in fact better than the therapeutic efficacy of anti-RSV drug ribavirin, which is currently in clinical use. It should be noted that to enhance the cell penetration and to increase the nuclease stability, the

DNA enzymes used in these studies were modified with PS units at both ends and a cholesterol moiety at the 3′-end. With these encouraging results in hand, the researchers tested the efficacy of the anti-RSV DNA enzyme in RSV-infected mice (Yang et al. 2007). Intranasal delivery of DNA enzyme resulted in a dose-dependent (0.2–0.8 mg) antiviral effect without producing any toxicity. RT-PCR assays have shown that the observed 54% mRNA reduction was a result of the DNA enzyme treatment. It would be interesting to see clinical tests of anti-RSV DNA enzymes because the results could be directly compared to an anti-RSV siRNA, which is currently in clinical trials (Meyers et al. 2009).

The ability of DNA enzymes to target the genomic RNA of Japanese encephalitis virus (JEV) has been demonstrated in in vitro and in vivo settings (Appaiahgari and Vrati 2007). Researchers designed a 10-23 DNA enzyme, which targets two direct repeat sequences located at the 3′-noncoding region (3′-NCR) of JEV virus. The 3′-NCR plays a crucial role in the replication of JEV. Both unmodified and completely PS-modified enzymes were used in these studies. Moreover, to enable the site-specific delivery to cells bearing scavenger receptors (ScRs), ten deoxyguanosine (poly-dG) residues were conjugated to the 3′-end of the unmodified and PS-modified enzymes. The in vitro cleavage assays under multiple turnover conditions in the presence of 2 mM Mg^{2+} (50 mM Tris–HCl, pH 7.5 at 37°C) revealed efficient cleavage of the 582-nt 3′-NCR sequence of JEV. It was also demonstrated that the poly-dG-modified DNA was taken up by murine macrophage cells, J744E. When tested for halting the JEV replication, the PS-modified DNA enzymes conjugated with poly-dG at the 3′-end showed 108-fold reductions of JEV replication (virus titers) at 5 μM enzyme concentrations. However, the randomized control DNA enzymes did not show any reduction in JEV titers supporting the specificity of DNA enzyme-mediated action. With these encouraging in vitro results in hand, researchers directly injected DNA enzymes (500 pmol) into JEV-infected mouse brains. After 72 h, the analysis of brain tissues revealed that the treatment with PS-modified DNA enzyme containing a PS-modified poly-dG tail resulted in 873-fold reduction in JEV titers. However, the unmodified DNA enzyme or a DNA enzyme control containing a randomized catalytic region did not show any substantial effect on JEV replication. Dose-dependent reduction of viral titers has also been reported in these studies. Injection of 1,000 pmol of completely PS-modified enzyme led to 99.99% of viral inhibition. The authors demonstrated the remarkable curing ability of DNA enzymes in mice infected with lethal JEV infection. These results clearly underscore the potential of RNA-cleaving DNA enzyme to treat viral infections of brain. Future studies are certainly warranted toward the realization of the clinical utility of these enzymes.

In order to target the translation initiation site (AUG) of influenza virus A, 10-23 DNA enzymes have been designed with varying binding arm lengths (7–9 nt) (Takahashi et al. 2004). To impart nuclease resistance, one or two N3′–P5′ phosphoramidate linkages (Fig. 4) have been introduced at the 3′- and 5′-ends of the enzymes. The kinetic evaluation of in vitro target cleavage using a 25-nt short RNA substrate under 25 mM Mg^{2+} (50 mM Tris–HCl, pH 7.5 at 37°C) has been

carried under multiple turnover conditions. The DNA enzyme with 9-nt binding arms and two N3′–P5′ phosphoramidate linkages at the 3′- and 5′-ends exhibited high catalytic efficiency [$k_{cat}/K_m = 1 \times 10^6$ (mol/L)$^{-1}$ min^{-1}], which was comparable to that of unmodified enzyme. When tested for the effect on viral replication in MDCK cells infected with influenza virus, the end-modified enzyme has shown 99% inhibition of virus. However, the in vitro inactive DNA enzyme controls also exhibited 49–58% inhibitory activity which points toward the contribution from the antisense mode of action.

An attempt to find viable strategies to address deadly severe acute respiratory syndrome-associated coronavirus (SARS-CoV), 10-23 DNA enzymes have been designed to target the 5′-UTR of a highly conserved fragment in the SARS genome (Wu et al. 2007). DNA enzyme having 9-nt binding arms was used to test the target cleavage efficacy on a 1-kb RNA transcript in in vitro settings. Under single turnover conditions and in the presence of 10 mM Mg^{2+}(50 mM Tris–HCl, pH 7.5 at 37°C), the 10-23 enzyme exhibited a k_{obs} of 0.064 min^{-1}. Under multiple turnover conditions, the initial velocity of the cleavage reaction was found to be 0.4 nM min^{-1}. Mutant enzymes did not show any significant cleavage under these conditions. Cellular efficacy of the DNA enzyme was evaluated using a SARS-CoV 5′-UTR-eGFP fusion plasmid in Vero E6 cells. FACS analysis revealed dose-dependent target attenuation (55–85%) of DNA enzyme-treated cells, while the mutant enzyme was found to be completely inactive. These results were further confirmed by RT-PCR analysis.

The effects of chemical modifications (2′-OMe, LNA, PS, etc.) in the binding arms and in the catalytic core of 10-23 DNA enzymes were investigated on deoxyribozymes targeting the 5′-UTR of human rhinovirus 14 (HRV14) (Schubert et al. 2003). The HRV14 is one of the viruses responsible for common cold. In vitro cleavage studies have been carried out using a 835-nt RNA transcript, which encodes the HRV14 genome. Both single turnover and multiple turnover experiments were performed in the presence of 10 mM Mg^{2+} (50 mM Tris–HCl, pH 7.5 at 37°C), and the respective rate constant (k_{obs}) and initial velocity (v_{init}) were determined to assess the catalytic potential. The cleavage assays revealed that DNA enzymes with 9-nt binding arms and four 2′-OMe or four LNA modifications on each binding arms were able to enhance the k_{obs} by factors of 2 and 4, respectively. Under multiple turnover conditions, the 2′-OMe-modified enzyme exhibited a sixfold enhancement in initial velocity, while the LNA-modified enzyme had shown a severe deceleration. The adverse effects of LNA-modified enzyme have been attributed to the high target binding, which influences the product release. The presence of PS modification in the binding arms severely affected the target cleavage under single and multiple turnover conditions. This can be attributed to the poor target recognition capabilities of PS modification. When the binding arms were shortened to 7 nt, the k_{obs} and v_{init} were drastically increased to several fold for 2′-OMe- and LNA-modified enzymes. For example, an enzyme with 7-nt binding arms having five 2′-OMe modifications on each arm enhanced the cleavage activity by 20-fold ($k_{obs} = 0.5$ min^{-1} and $v_{init} = 4.7$ nM min^{-1}) compared to the unmodified counterpart. Researchers also tried to evaluate the effect of

2′-OMe modification in the 15-nt catalytic core of the 10-23 DNA enzyme. Systematic replacement of each nucleotide in the catalytic core with 2′-OMe modification led to the identification of six positions (2, 7, 8, 11, 14, and 15), which are amenable to the modifications without losing the cleavage efficiency. This is one of the very few reports in which chemical modifications have been successfully utilized in the catalytic core of 10-23 enzyme. To address the nuclease vulnerability of DNA enzymes in cellular environment, an optimized DNA enzyme with 7-nt binding arms containing five 2′-OMe modifications on each binding arm and six 2′-OMe modifications in the catalytic core has been designed. This highly engineered DNA enzyme had an impressive cleavage potential, which is indicated by a tenfold increase in the k_{obs} (0.57 min^{-1}) and v_{init} (2 nM min^{-1}) compared to the unmodified enzyme. The enzyme exhibited a half-life of 25 h in 10% fetal calf serum. Though these results are promising from the therapeutic point of view, unfortunately, the potential of this modified enzyme to cleave the RNA target of HRV14 in cellular systems is not reported in the literature. In a related study, researchers demonstrated the potential of using 2′-OMe or LNA modification on the binding arms of DNA enzymes to cleave inaccessible targets present in the 5′-UTR of coxsackievirus (CAV-21) (Schubert et al. 2004). In spite of the fact that the target site in the CAV-21 shares sequence homology with the 5′-UTR of HRV-14, unmodified DNA enzyme in the presence of 10 mM Mg^{2+} (50 mM Tris–HCl, pH 7.0 at 37°C) could not impart the cleavage of a 797-nt CAV-21 transcript. This shows that target sequences in HRV-14 and CAV-21 do not share similar accessibility features for DNA enzyme-promoted cleavage. However, when the 7-nt binding arms of the enzyme were modified with five 2′-OMe or three LNA moieties, complete cleavage of the target was observed under single turnover conditions. These studies point toward the need to perform thorough target accessibility studies while designing DNA enzymes against the conserved regions of mRNAs belonging to different organisms.

5.3 Delivery Strategies for DNA Enzymes

In order to capitalize the full therapeutic potential of RNA-cleaving DNA enzymes, the use of in vivo delivery agents is warranted. Unfortunately, only a handful of reports exist in the literature dealing with the DNA enzyme delivery issue (Tan et al. 2009b). The first study on deoxyribozyme delivery used DNA enzymes encapsulated in microspheres made of poly(lactic acid) and poly (glycolic acid) (PLGA) to target EGFR mRNA (Khan et al. 2004). Although these studies demonstrated the ability of sustained release of DNA enzymes in vitro, the effect on the target gene downregulation and the amount of DNA enzyme encapsulated in microspheres were not reported. To deliver anti-*c-MYC* DNA enzymes to subcutaneous tumors in mice, nanoparticles based on linear polymers of cyclodextrin complexed with DNA enzymes (termed “polyplexes”) have been used (Pun et al. 2004). In order to enhance the surface properties and to

harness receptor-mediated delivery into tumor cells, polyplexes were modified with polyethylene glycol and transferrin (Tf-PEG-polyplex). Transferrin is an iron-containing protein whose receptor is highly expressed in tumor cells. Intravenous and intraperitoneal injection of Tf-PEG-polyplexes containing fluorescently tagged DNA enzymes resulted in the maximum accumulation of the DNA enzymes in tumor sites. However, the toxicity profiles of the Tf-PEG-polyplexes and the capability of the delivered DNA enzymes to reduce the tumor volume have not been reported in this study.

Poly(propylene imine) dendrimers have also been used for the in vitro and in vivo delivery of DNA enzymes. DNA enzymes complexed with cationic dendrimers showed >80% transfection efficiency in carcinoma A2780 cells (Tack et al. 2006). Moreover, intravenous injection of fluorescently labeled dendrimer–DNA enzyme complexes into ovarian carcinoma-bearing mice resulted in the accumulation of DNA enzymes in the tumor and also in the cell nucleus. When tested for toxicity, the DNA enzyme–dendrimer complexes showed minimal toxicity. It should be noted that toxicity profiles of these complexes in noncancerous cell lines have not been reported so far. Moreover, the gene silencing activity of the DNA enzymes delivered using cationic dendrimers has not been confirmed. This demands more studies on these delivery agents before they can make their way to clinical trials. The use of gold nanoparticles linked with cationic polymers (polylysine/polyethylamine) and transferrin has been reported for the delivery of DNA enzymes targeting *c-MYC* in HT-29 colon carcinoma cells (Tack et al. 2008). Varying transfection efficiencies (43–77%) were reported based on the nature of the cationic polymers used. No further studies have so far been reported on the toxicity profile of this gold nanoparticle-based delivery system as well as the in vivo efficacy of mRNA downregulation.

The most promising DNA enzyme delivery strategy reported in the literature is nanoparticles made of the carbohydrate-based biopolymer chitosan and DNA enzymes (Tan et al. 2009a). These chitosan-based nanoparticles were used to deliver the *c-JUN*-targeting DNA enzyme Dz13 to osteosarcoma cells SaOS-2 (Tan et al. 2010). Dz13-mediated apoptosis was evident in these studies. Further studies in tumor-bearing mice models demonstrated nontoxicity and the power of the chitosan-Dz13 nanoparticles to treat the osteosarcoma efficiently. Though these results are highly encouraging, it is difficult to predict whether chitosan-based delivery systems may once be used for the delivery of DNA enzymes targeting viral, cardiovascular, and other cancer targets. Moreover, the true clinical utility of this delivery system has yet to be investigated.

5.4 *Challenges and Opportunities for DNA Enzyme-Based Therapeutics*

In the last 12 years, there has been considerable progress in DNA enzyme research, which has been devoted to the development of deoxyribozymes as therapeutic

agents against various deadly diseases as well as against viral and bacterial pathogens. These efforts include attempts to impart nuclease stability and enhance the target accessibility, specificity, and target binding affinity by introducing various chemical modifications in the binding arms and in the catalytic core of DNA enzymes. The chemical modifications are more or less well tolerated in the binding arms, but they are found to be less tolerated in the catalytic core (see above Sect. 4). To impart endonucleolytic resistance, incorporation of modifications in the catalytic core will be beneficial (Schubert et al. 2003). The search for an ideal chemical modification which is capable of imparting all desired therapeutic properties to DNA enzyme is far from over. It should also be emphasized that most of the studies in this direction have been directed to chemically fine-tune 10-23 DNA enzyme perhaps owing to its early known high in vitro cleavage efficacy on any purine–pyrimidine RNA junction. The discovery of the large family of 8-17 DNA enzymes which are capable of practically cleaving any dinucleotide RNA junction (Cruz et al. 2004) should encourage researchers to evaluate the therapeutic utility of these short DNA catalysts as well.

One of the important aspects which was not explored completely with respect to therapeutic development is the in vitro selection of new chemically modified RNA-cleaving DNA enzymes, which are tailored with functionalities that are capable of imparting drug-like properties. The nonavailability of a universal DNA polymerase which can incorporate sugar-, base-, and/or backbone-modified nucleoside triphosphates into a growing DNA chain poses major challenges to such efforts. Though attempts to select metal ion-independent DNA enzymes using chemically modified triphosphates have been carried out, the evolved enzymes were found to be less superior in their cleavage efficiency compared to 10-23 and 8-17 enzymes (Santoro et al. 2000; Sidorov et al. 2004; Ting et al. 2004; Hollenstein et al. 2009). The rationale behind these studies has been the fact that both 10-23 and 8-17 require high Mg^{2+} (>5 mM) for very efficient in vitro RNA cleavage. This concentration is far from the physiological Mg^{2+} concentration (0.2–0.8 mM). However, the available data on the excellent cleavage activity of 10-23 enzymes in cellular systems and in animal models demonstrate that therapeutically demanding target cleavage can indeed be achieved with the help of known enzymes. If one wants to really improve the in vivo efficiency, it may be desirable to evolve new RNA-cleaving enzymes under physiologically relevant metal ion concentrations. Another possibility is to perform in vitro selection experiments in conditions mimicking the cellular environment analogous to efforts which have been undertaken for the in vitro selection of cell-specific aptamers (Raddatz et al. 2008).

Off-target effects of DNA enzymes have not been widely investigated unlike in the case of antisense oligonucleotides and siRNAs. Recently, it has been reported that some DNA enzymes such as Dz13, which was earlier reported for therapeutic action on a wide range of tumors, are actually promoting apoptosis due to the activation of inhibitor of caspase-activated deoxyribonuclease and protein kinase C delta (Dass et al. 2010). The sequence composition of the DNA enzyme can also impart unwanted toxicity. DNA enzymes which are rich in Gs have been shown to enhance cytotoxic effects (Goodchild et al. 2007). These results are alarming and

demand for more rigorous off-target/toxicity profiling of any DNA enzyme which is slated for in vivo use. At the delivery front, DNA enzyme therapeutics may benefit from the major research efforts which are currently under way for antisense oligonucleotides and siRNAs (Stanton and Colletti 2010).

6 Conclusions and Future Perspectives

In summary, artificial single-stranded DNA enzymes can serve as useful tools for the site-specific cleavage of RNA for various applications. Seventeen years after the initial report, this intriguing property of DNA is still of conceptual interest with respect to exploring the general catalytic ability and potential limitations of DNA enzymes. The basic mechanistic principles of DNA-catalyzed scission of RNA phosphodiester bonds have been studied by biochemical methods, and the DNA folding processes have been explored by biophysical approaches. Nevertheless, the molecular details of how such impressive rate enhancements of up to 10^8-fold are achieved are far from being fully understood. Clearly, more biochemical and structural data are needed to disentangle the contributions of individual nucleotides, metal ions, and water molecules in the active sites of DNA catalysts.

With respect to applications as therapeutic agents, the efficiency of DNA catalysts compares well with other nucleic acid-based strategies to downregulate protein expression, but, at the same time, faces similar difficulties as well. However, unlike in the case of other DNA- or RNA-based therapeutic agents, detailed pharmacokinetic and pharmacodynamic studies are yet to be conducted for RNA-cleaving DNA enzymes. To increase the in vivo efficiency, promising developments can currently be found in recent in vitro selection attempts that strive to improve the tolerance for low divalent metal ion concentrations by expanding the chemical diversity of DNA nucleotides. Modified nucleotide modifications will also serve effectively for enhancing the lifetime of DNA enzymes under the demanding conditions encountered in biological environments. Together with modern strategies for delivery of modified DNA enzymes, it can be expected that deoxyribozymes may find their way to clinic in the near future. Even though RNA-cleaving DNA enzymes have not yet made it to real-life therapeutic applications, they have been serving the scientific community as valuable research tools to address biochemical, biomedical, and bioanalytical problems.

Acknowledgments Financial support from Department of Science and Technology (DST), Government of India (FAST track scheme, SR/FT/LS-133/2008) to P.I.P. is gratefully acknowledged. C.H. is supported by the Max Planck Society, and P.I.P. is a recipient of a Max-Planck India Fellowship (MPG-DST scheme).

References

Achenbach JC, Chiuman W, Cruz RP et al (2004) DNAzymes: from creation in vitro to application in vivo. Curr Pharm Biotechnol 5:321–336

Appaiahgari MB, Vrati S (2007) DNAzyme-mediated inhibition of Japanese encephalitis virus replication in mouse brain. Mol Ther 15:1593–1599

Bano AS, Gupta N, Sharma Y et al (2007) HIV-1 VprB and C RNA cleavage by potent 10-23 DNAzymes that also cause reversal of G2 cell cycle arrest mediated by Vpr genes. Oligonucleotides 17:465–472

Basu S, Sriram B, Goila R et al (2000) Targeted cleavage of HIV-1 coreceptor-CXCR-4 by RNA-cleaving DNA-enzyme: inhibition of coreceptor function. Antiviral Res 46:125–134

Baum DA, Silverman SK (2008) Deoxyribozymes: useful DNA catalysts in vitro and in vivo. Cell Mol Life Sci 65:2156–2174

Benson VL, Khachigian LM, Lowe HC (2008) DNAzymes and cardiovascular disease. Br J Pharmacol 154:741–748

Bhindi R, Fahmy RG, Lowe HC et al (2007) Brothers in arms: DNA enzymes, short interfering RNA, and the emerging wave of small-molecule nucleic acid-based gene-silencing strategies. Am J Pathol 171:1079–1088

Breaker RR (2004) Natural and engineered nucleic acids as tools to explore biology. Nature 432:838–845

Breaker RR, Joyce GF (1994) A DNA enzyme that cleaves RNA. Chem Biol 1:223–229

Breaker RR, Joyce GF (1995) A DNA enzyme with Mg^{2+}-dependent RNA phosphodiesterase activity. Chem Biol 2:655–660

Burmeister J, von Kiedrowski G, Ellington AD (1997) Cofactor-assisted self-cleavage in DNA Libraries with a 3′-5′ phosphoramidate bond. Angew Chem Int Ed 36:1321–1324

Carmi N, Balkhi SR, Breaker RR (1998) Cleaving DNA with DNA. Proc Natl Acad Sci USA 95:2233–2237

Chakraborti S, Banerjea AC (2003) Inhibition of HIV-1 gene expression by novel DNA enzymes targeted to cleave HIV-1 TAR RNA: potential effectiveness against all HIV-1 isolates. Mol Ther 7:817–826

Chandra M, Silverman SK (2008) DNA and RNA can be equally efficient catalysts for carbon-carbon bond formation. J Am Chem Soc 130:2936–2937

Chandra M, Sachdeva A, Silverman SK (2009) DNA-catalyzed sequence-specific hydrolysis of DNA. Nat Chem Biol 5:718–720

Chen F, Li Z, Wang R et al (2004a) Inhibition of ampicillin-resistant bacteria by novel mono-DNAzymes and di-DNAzyme targeted to beta-lactamase mRNA. Oligonucleotides 14:80–89

Chen F, Wang R, Li Z et al (2004b) A novel replicating circular DNAzyme. Nucleic Acids Res 32:2336–2341

Chinnapen DJ, Sen D (2004) A deoxyribozyme that harnesses light to repair thymine dimers in DNA. Proc Natl Acad Sci U S A 101:65–69

Choi YJ, Han HJ, Lee JH et al (2000) Synthesis and NMR studies of the RNA-cleaving DNA enzyme. B Kor Chem Soc 21:955–956

Cieslak M, Szymanski J, Adamiak RW et al (2003) Structural rearrangements of the 10-23 DNAzyme to beta 3 integrin subunit mRNA induced by cations and their relations to the catalytic activity. J Biol Chem 278:47987–47996

Coppins RL, Silverman SK (2004) A DNA enzyme that mimics the first step of RNA splicing. Nat Struct Mol Biol 11:270–274

Cruz RPG, Withers JB, Li Y (2004) Dinucleotide junction cleavage versatility of 8-17 deoxyribozyme. Chem Biol 11:57–67

Dash BC, Banerjea AC (2004) Sequence-specific cleavage activities of DNA enzymes targeted against HIV-1 Gag and Nef regions. Oligonucleotides 14:41–47

Dass CR, Choong PF, Khachigian LM (2008) DNAzyme technology and cancer therapy: cleave and let die. Mol Cancer Ther 7:243–251

Dass CR, Tan ML, Galloway SJ et al (2010) Dz13 induces a cytotoxic stress response with upregulation of E2F1 in tumor cells metastasizing to or from bone. Oligonucleotides 20:79–91
Donini S, Clerici M, Wengel J et al (2007) The advantages of being locked. Assessing the cleavage of short and long RNAs by locked nucleic acid-containing 8-17 deoxyribozymes. J Biol Chem 282:35510–35518
Doudna JA, Cech TR (2002) The chemical repertoire of natural ribozymes. Nature 418:222–228
Faulhammer D, Famulok M (1996) The Ca^{2+} ion as a cofactor for a novel RNA-cleaving deoxyribozyme. Angew Chem Int Ed Engl 35:2837–2841
Feldman AR, Sen D (2001) A new and efficient DNA enzyme for the sequence-specific cleavage of RNA. J Mol Biol 313:283–294
Frederiksen JK, Piccirilli JA (2009) Identification of catalytic metal ion ligands in ribozymes. Methods 49:146–166
Geyer CR, Sen D (1997) Evidence for the metal-cofactor independence of an RNA phosphodiester-cleaving DNA enzyme. Chem Biol 4:579–593
Geyer CR, Sen D (1998) Lanthanide probes for a phosphodiester-cleaving, lead-dependent, DNAzyme. J Mol Biol 275:483–489
Goila R, Banerjea AC (1998) Sequence specific cleavage of the HIV-1 coreceptor CCR5 gene by a hammer-head ribozyme and a DNA-enzyme: inhibition of the coreceptor function by DNA-enzyme. FEBS Lett 436:233–238
Goila R, Banerjea AC (2001) Inhibition of hepatitis B virus X gene expression by novel DNA enzymes. Biochem J 353:701–708
Goodchild A, King A, Gozar MM et al (2007) Cytotoxic G-rich oligodeoxynucleotides: putative protein targets and required sequence motif. Nucleic Acids Res 35:4562–4572
Guerrier-Takada C, Gardiner K, Marsh T et al (1983) The RNA moiety of ribonuclease P is the catalytic subunit of the enzyme. Cell 35:849–857
He QC, Zhou JM, Zhou DM et al (2002) Comparison of metal-ion-dependent cleavages of RNA by a DNA enzyme and a hammerhead ribozyme. Biomacromolecules 3:69–83
He J, Zhang D, Wang Q et al (2011) A novel strategy of chemical modification for rate enhancement of 10-23 DNAzyme: a combination of A9 position and 8-aza-7-deaza-2′-deoxyadenosine analogs. Org Biomol Chem 9:5728–5736
Höbartner C, Pradeepkumar PI, Silverman SK (2007) Site-selective depurination by a periodate-dependent deoxyribozyme. Chem Commun:2255–2257
Hollenstein M, Hipolito CJ, Lam CH et al (2009) A self-cleaving DNA enzyme modified with amines, guanidines and imidazoles operates independently of divalent metal cations (M2+). Nucleic Acids Res 37:1638–1649
Hou W, Ni Q, Wo J et al (2006) Inhibition of hepatitis B virus X gene expression by 10-23 DNAzymes. Antiviral Res 72:190–196
Hou Z, Meng JR, Zhao JR et al (2007) Inhibition of beta-lactamase-mediated oxacillin resistance in *Staphylococcus aureus* by a deoxyribozyme. Acta Pharmacol Sin 28:1775–1782
Jakobsen MR, Haasnoot J, Wengel J et al (2007) Efficient inhibition of HIV-1 expression by LNA modified antisense oligonucleotides and DNAzymes targeted to functionally selected binding sites. Retrovirology 4:29
Joyce GF (2004) Directed evolution of nucleic acid enzymes. Annu Rev Biochem 73:791–836
Joyce GF (2007) Forty years of in vitro evolution. Angew Chem Int Ed Engl 46:6420–6436
Kenward M, Dorfman KD (2009) Coarse-grained brownian dynamics simulations of the 10-23 DNAzyme. Biophys J 97:2785–2793
Khan A, Benboubetra M, Sayyed PZ et al (2004) Sustained polymeric delivery of gene silencing antisense ODNs, siRNA, DNAzymes and ribozymes: in vitro and in vivo studies. J Drug Target 12:393–404
Kim HK, Liu J, Li J et al (2007a) Metal-dependent global folding and activity of the 8-17 DNAzyme studied by fluorescence resonance energy transfer. J Am Chem Soc 129:6896–6902
Kim HK, Rasnik I, Liu J et al (2007b) Dissecting metal ion-dependent folding and catalysis of a single DNAzyme. Nat Chem Biol 3:763–768

Kim HK, Li J, Nagraj N et al (2008) Probing metal binding in the 8-17 DNAzyme by TbIII luminescence spectroscopy. Chemistry 14:8696–8703
Kost DM, Gerdt JP, Pradeepkumar PI et al (2008) Controlling the direction of site-selectivity and regioselectivity in RNA ligation by Zn2+-dependent deoxyribozymes that use 2′,3′-cyclic phosphate RNA substrates. Org Biomol Chem 6:4391–4398
Kruger K, Grabowski PJ, Zaug AJ et al (1982) Self-splicing RNA: autoexcision and autocyclization of the ribosomal RNA intervening sequence of Tetrahymena. Cell 31:147–157
Lam JC, Li Y (2010) Influence of cleavage site on global folding of an RNA-cleaving DNAzyme. Chembiochem 11:1710–1719
Lee NK, Koh HR, Han KY et al (2007) Folding of 8-17 deoxyribozyme studied by three-color alternating-laser excitation of single molecules. J Am Chem Soc 129:15526–15534
Lee NK, Koh HR, Han KY et al (2010) Single-molecule, real-time measurement of enzyme kinetics by alternating-laser excitation fluorescence resonance energy transfer. Chem Commun 46:4683–4685
Lee CS, Mui TP, Silverman SK (2011) Improved deoxyribozymes for synthesis of covalently branched DNA and RNA. Nucleic Acids Res 39:269–279
Leung EK, Suslov N, Tuttle N et al (2011) The mechanism of peptidyl transfer catalysis by the ribosome. Annu Rev Biochem 80:527–555
Levy M, Ellington AD (2001) Selection of deoxyribozyme ligases that catalyze the formation of an unnatural internucleotide linkage. Bioorg Med Chem 9:2581–2587
Li Y, Breaker RR (1999) Phosphorylating DNA with DNA. Proc Natl Acad Sci USA 96:2746–2751
Li Y, Sen D (1996) A catalytic DNA for porphyrin metallation. Nat Struct Biol 3:743–747
Li J, Zheng W, Kwon AH, Lu Y (2000a) In vitro selection and characterization of a highly efficient Zn(II)-dependent RNA-cleaving deoxyribozyme. Nucleic Acids Res 28:481–488
Li Y, Liu Y, Breaker RR (2000b) Capping DNA with DNA. Biochemistry 39:3106–3114
Li J, Zhu D, Yi Z et al (2005) DNAzymes targeting the icl gene inhibit ICL expression and decrease *Mycobacterium tuberculosis* survival in macrophages. Oligonucleotides 15:215–222
Li J, Wang N, Luo Q et al (2010) The 10-23 DNA enzyme generated by a novel expression vector mediate inhibition of taco expression in macrophage. Oligonucleotides 20:61–68
Lilley DM (2011) Catalysis by the nucleolytic ribozymes. Biochem Soc Trans 39:641–646
Liu Y, Sen D (2008) A contact photo-cross-linking investigation of the active site of the 8-17 deoxyribozyme. J Mol Biol 381:845–859
Liu Y, Sen D (2010) Local rather than global folding enables the lead-dependent activity of the 8-17 deoxyribozyme: evidence from contact photo-crosslinking. J Mol Biol 395:234–241
Liu Z, Mei SH, Brennan JD et al (2003) Assemblage of signaling DNA enzymes with intriguing metal-ion specificities and pH dependences. J Am Chem Soc 125:7539–7545
Liu J, Brown AK, Meng X et al (2007) A catalytic beacon sensor for uranium with parts-per-trillion sensitivity and millionfold selectivity. Proc Natl Acad Sci U S A 104:2056–2061
Meyers R, Alvarez R, Elbashir S et al (2009) RNA interference-mediated silencing of the respiratory syncytial virus nucleocapsid defines a potent antiviral strategy. Antimicrob Agents Chemother 53:3952–3962
Nawrot B, Widera K, Wojcik M et al (2007) Mapping of the functional phosphate groups in the catalytic core of deoxyribozyme 10-23. FEBS J 274:1062–1072
Nawrot B, Widera K, Sobczak M et al (2008) Effect of R-P and S(P)phosphorothioate substitution at the scissile site on the cleavage activity of deoxyribozyme 10-23. Curr Org Chem 12:1004–1009
Nowakowski J, Shim PJ, Prasad GS et al (1999) Crystal structure of an 82-nucleotide RNA-DNA complex formed by the 10-23 DNA enzyme. Nat Struct Biol 6:151–156
Oketani M, Asahina Y, Wu CH et al (1999) Inhibition of hepatitis C virus-directed gene expression by a DNA ribonuclease. J Hepatol 31:628–634

Pearson AM, Rich A, Krieger M (1993) Polynucleotide binding to macrophage scavenger receptors depends on the formation of base-quartet-stabilized four-stranded helices. J Biol Chem 268:3546–3554

Peracchi A (2000) Preferential activation of the 8-17 deoxyribozyme by Ca^{2+} ions. Evidence for the identity of 8-17 with the catalytic domain of the Mg5 deoxyribozyme. J Biol Chem 275:11693–11697

Peracchi A (2004) Prospects for antiviral ribozymes and deoxyribozymes. Rev Med Virol 14:47–64

Peracchi A, Bonaccio M, Clerici M (2005) A mutational analysis of the 8-17 deoxyribozyme core. J Mol Biol 352:783–794

Pradeepkumar PI, Höbartner C, Baum DA et al (2008) DNA-catalyzed formation of nucleopeptide linkages. Angew Chem Int Ed 47:1753–1757

Pun SH, Tack F, Bellocq NC et al (2004) Targeted delivery of RNA-cleaving DNA enzyme (DNAzyme) to tumor tissue by transferrin-modified, cyclodextrin-based particles. Cancer Biol Ther 3:641–650

Purtha WE, Coppins RL, Smalley MK et al (2005) General deoxyribozyme-catalyzed synthesis of native 3′-5′ RNA linkages. J Am Chem Soc 127:13124–13125

Pyle AM, Chu VT, Jankowsky E et al (2000) Using DNAzymes to cut, process, and map RNA molecules for structural studies or modification. Methods Enzymol 317:140–146

Raddatz MS, Dolf A, Endl E et al (2008) Enrichment of cell-targeting and population-specific aptamers by fluorescence-activated cell sorting. Angew Chem Int Ed Engl 47:5190–5193

Reyes-Gutierrez P, Alvarez-Salas LM (2009) Cleavage of HPV-16 E6/E7 mRNA mediated by modified 10-23 deoxyribozymes. Oligonucleotides 19:233–242

Robaldo L, Montserrat JM, Iribarren AM (2010) 10-23 DNAzyme modified with (2′R)- and (2′S)-2′-deoxy-2′-C-methyluridine in the catalytic core. Bioorg Med Chem Lett 20:4367–4370

Roth A, Breaker RR (1998) An amino acid as a cofactor for a catalytic polynucleotide. Proc Natl Acad Sci U S A 95:6027–6031

Roy S, Gupta N, Subramanian N et al (2008) Sequence-specific cleavage of hepatitis C virus RNA by DNAzymes: inhibition of viral RNA translation and replication. J Gen Virol 89:1579–1586

Santoro SW, Joyce GF (1997) A general purpose RNA-cleaving DNA enzyme. Proc Natl Acad Sci U S A 94:4262–4266

Santoro SW, Joyce GF (1998) Mechanism and utility of an RNA-cleaving DNA enzyme. Biochemistry 37:13330–13342

Santoro SW, Joyce GF, Sakthivel K et al (2000) RNA cleavage by a DNA enzyme with extended chemical functionality. J Am Chem Soc 122:2433–2439

Schlosser K, Li Y (2009a) Biologically inspired synthetic enzymes made from DNA. Chem Biol 16:311–322

Schlosser K, Li Y (2009b) DNAzyme-mediated catalysis with only guanosine and cytidine nucleotides. Nucleic Acids Res 37:413–420

Schlosser K, Li Y (2010) A versatile endoribonuclease mimic made of DNA: characteristics and applications of the 8-17 RNA-cleaving DNAzyme. Chembiochem 11:866–879

Schlosser K, Gu J, Lam JC et al (2008a) In vitro selection of small RNA-cleaving deoxyribozymes that cleave pyrimidine-pyrimidine junctions. Nucleic Acids Res 36:4768–4777

Schlosser K, Gu J, Sule L et al (2008b) Sequence-function relationships provide new insight into the cleavage site selectivity of the 8-17 RNA-cleaving deoxyribozyme. Nucleic Acids Res 36:1472–1481

Schubert S, Gul DC, Grunert HP et al (2003) RNA cleaving '10-23' DNAzymes with enhanced stability and activity. Nucleic Acids Res 31:5982–5992

Schubert S, Furste JP, Werk D et al (2004) Gaining target access for deoxyribozymes. J Mol Biol 339:355–363

Sheppard TL, Ordoukhanian P, Joyce GF (2000) A DNA enzyme with *N*-glycosylase activity. Proc Natl Acad Sci U S A 97:7802–7807

Sidorov AV, Grasby JA, Williams DM (2004) Sequence-specific cleavage of RNA in the absence of divalent metal ions by a DNAzyme incorporating imidazolyl and amino functionalities. Nucleic Acids Res 32:1591–1601

Silverman SK (2005) In vitro selection, characterization, and application of deoxyribozymes that cleave RNA. Nucleic Acids Res 33:6151–6163

Silverman SK (2008) Catalytic DNA (deoxyribozymes) for synthetic applications-current abilities and future prospects. Chem Commun:3467–3485

Silverman SK (2009) Deoxyribozymes: selection design and serendipity in the development of DNA catalysts. Acc Chem Res 42:1521–1531

Silverman SK (2010) DNA as a versatile chemical component for catalysis, encoding, and stereocontrol. Angew Chem Int Ed 49:7180–7201

Silverman SK, Baum DA (2009) Use of deoxyribozymes in RNA research. Methods Enzymol 469:95–117

Sood V, Gupta N, Bano AS et al (2007a) DNA-enzyme-mediated cleavage of human immunodeficiency virus type 1 Gag RNA is significantly augmented by antisense-DNA molecules targeted to hybridize close to the cleavage site. Oligonucleotides 17:113–121

Sood V, Unwalla H, Gupta N et al (2007b) Potent knock down of HIV-1 replication by targeting HIV-1 Tat/Rev RNA sequences synergistically with catalytic RNA and DNA. AIDS 21:31–40

Sriram B, Banerjea AC (2000) In vitro-selected RNA cleaving DNA enzymes from a combinatorial library are potent inhibitors of HIV-1 gene expression. Biochem J 352(Pt 3):667–673

Stanton MG, Colletti SL (2010) Medicinal chemistry of siRNA delivery. J Med Chem 53:7887–7901

Sugimoto N, Okumoto Y, Ohmichi T (1999) Effect of metal ions and sequence of deoxyribozymes on their RNA cleavage activity. J Chem Soc Perkin Trans 2:1381–1386

Tack F, Bakker A, Maes S et al (2006) Modified poly(propylene imine) dendrimers as effective transfection agents for catalytic DNA enzymes (DNAzymes). J Drug Target 14:69–86

Tack F, Noppe M, Van Dijck A et al (2008) Delivery of a DNAzyme targeting c-myc to HT29 colon carcinoma cells using a gold nanoparticulate approach. Pharmazie 63:221–225

Takahashi H, Hamazaki H, Habu Y et al (2004) A new modified DNA enzyme that targets influenza virus A mRNA inhibits viral infection in cultured cells. FEBS Lett 560:69–74

Tan XX, Rose K, Margolin W et al (2004) DNA enzyme generated by a novel single-stranded DNA expression vector inhibits expression of the essential bacterial cell division gene ftsZ. Biochemistry 43:1111–1117

Tan ML, Choong PF, Dass CR (2009a) Cancer, chitosan nanoparticles and catalytic nucleic acids. J Pharm Pharmacol 61:3–12

Tan ML, Choong PF, Dass CR (2009b) DNAzyme delivery systems: getting past first base. Expert Opin Drug Deliv 6:127–138

Tan ML, Dunstan DE, Friedhuber AM et al (2010) A nanoparticulate system that enhances the efficacy of the tumoricide Dz13 when administered proximal to the lesion site. J Control Release 144:196–202

Ting R, Thomas JM, Lermer L et al (2004) Substrate specificity and kinetic framework of a DNAzyme with an expanded chemical repertoire: a putative RNaseA mimic that catalyzes RNA hydrolysis independent of a divalent metal cation. Nucleic Acids Res 32:6660–6672

Travascio P, Li Y, Sen D (1998) DNA-enhanced peroxidase activity of a DNA-aptamer-hemin complex. Chem Biol 5:505–517

Trepanier J, Tanner JE, Momparler RL et al (2006) Cleavage of intracellular hepatitis C RNA in the virus core protein coding region by deoxyribozymes. J Viral Hepat 13:131–138

Trepanier JB, Tanner JE, Alfieri C (2008) Reduction in intracellular HCV RNA and virus protein expression in human hepatoma cells following treatment with 2′-O-methyl-modified anti-core deoxyribozyme. Virology 377:339–344

Unwalla H, Banerjea AC (2001a) Inhibition of HIV-1 gene expression by novel macrophage-tropic DNA enzymes targeted to cleave HIV-1 TAT/Rev RNA. Biochem J 357:147–155

Unwalla H, Banerjea AC (2001b) Novel mono- and di-DNA-enzymes targeted to cleave TAT or TAT-REV RNA inhibit HIV-1 gene expression. Antiviral Res 51:127–139
Unwalla H, Chakraborti S, Sood V et al (2006) Potent inhibition of HIV-1 gene expression and TAT-mediated apoptosis in human T cells by novel mono- and multitarget anti-TAT/Rev/Env ribozymes and a general purpose RNA-cleaving DNA-enzyme. Antiviral Res 72:134–144
Vester B, Hansen LH, Lundberg LB et al (2006) Locked nucleoside analogues expand the potential of DNAzymes to cleave structured RNA targets. BMC Mol Biol 7:19
Wachowius F, Höbartner C (2011) Probing essential nucleobase functional groups in aptamers and deoxyribozymes by nucleotide analogue interference mapping of DNA. J Am Chem Soc: ASAP
Wachowius F, Javadi-Zarnaghi F, Höbartner C (2010) Combinatorial mutation interference analysis reveals functional nucleotides required for DNA catalysis. Angew Chem Int Ed 49:8504–8508
Wang Y, Silverman SK (2005) Efficient one-step synthesis of biologically related lariat RNAs by a deoxyribozyme. Angew Chem Int Ed 44:5863–5866
Wang B, Cao L, Chiuman W et al (2010) Probing the function of nucleotides in the catalytic cores of the 8-17 and 10-23 DNAzymes by abasic nucleotide and C3 spacer substitutions. Biochemistry 49:7553–7562
Willner I, Shlyahovsky B, Zayats M et al (2008) DNAzymes for sensing, nanobiotechnology and logic gate applications. Chem Soc Rev 37:1153–1165
Wong OY, Pradeepkumar PI, Silverman SK (2011) DNA-catalyzed covalent modification of amino acid side chains in tethered and free peptide substrates. Biochemistry 50:4741–4749
Wu S, Xu J, Liu J et al (2007) An efficient RNA-cleaving DNA enzyme can specifically target the 5′-untranslated region of severe acute respiratory syndrome associated coronavirus (SARS-CoV). J Gene Med 9:1080–1086
Xie YY, Zhao XD, Jiang LP et al (2006) Inhibition of respiratory syncytial virus in cultured cells by nucleocapsid gene targeted deoxyribozyme (DNAzyme). Antiviral Res 71:31–41
Yang XQ, Zhou J, Xie YY et al (2007) Inhibition of respiratory syncytial virus of subgroups A and B using deoxyribozyme DZ1133 in mice. Virus Res 130:241–248
Zaborowska Z, Furste JP, Erdmann VA et al (2002) Sequence requirements in the catalytic core of the "10-23" DNA enzyme. J Biol Chem 277:40617–40622
Zaborowska Z, Schubert S, Kurreck J et al (2005) Deletion analysis in the catalytic region of the 10-23 DNA enzyme. FEBS Lett 579:554–558
Zhang X, Xu Y, Ling H et al (1999) Inhibition of infection of incoming HIV-1 virus by RNA-cleaving DNA enzyme. FEBS Lett 458:151–156